NACA RM No. 9A05

RESEARCH MEMORANDUM

DETERMINATION OF RATE, AREA, AND DISTRIBUTION OF IMPINGEMENT OF WATERDROPS ON VARIOUS AIRFOILS FROM TRAJECTORIES OBTAINED ON THE DIFFERENTIAL ANALYZER

By

A. G. Guibert, E. Janssen, and W. M. Robbins

University of California

NATIONAL ADVISORY COMMITTEE
FOR AERONAUTICS

WASHINGTON

February 16, 1949

NACA RM No. 9A05

NATIONAL ADVISORY COMMITTEE FOR AERONAUTICS

RESEARCH MEMORANDUM

DETERMINATION OF RATE, AREA, AND DISTRIBUTION OF IMPINGEMENT OF WATERDROPS ON VARIOUS AIRFOILS FROM TRAJECTORIES OBTAINED ON THE DIFFERENTIAL ANALYZER

By A. G. Guibert, E. Janssen, and W. M. Robbins

SUMMARY

The trajectories of waterdrops in air flowing over airfoils are determined for three airfoil - angle-of-attack combinations using the differential analyzer to solve the differential equations of motion of the waterdrops. From these trajectories the rate of water impingement, the area of impingement, and the distribution of impingement are determined as functions of two dimensionless moduli.

Comparisons are made of the rate of water impingement on these airfoils and the rate of water impingement on cylinders.

INTRODUCTION

If a body of any shape and size moves through a cloud, some of the waterdrops in its path will tend to impinge on the surface of that body over an area which will vary according to the size of the drops, the speed of the body, and so forth. Other drops originally in its path will be carried around the body and will not impinge. Studies have been made of the rate and distribution of impingement of waterdrops on cylinders and two different airfoils by means of numerical integration of the differential equations of the motion of the drops (references 1, 2, and 3) and on cylinders, spheres, and ribbons by solution of these equations on a differential analyzer (reference 4).

References 1 and 2 both made the assumption that the velocity and size of the drops were such that Stokes' law of resistance was followed. References 3 and 4 did not make this assumption, which is not applicable at the velocities of airplanes and for the drop sizes prevalent in clouds. These references employed instead the experimentally determined drag coefficient for spheres as a better approximation to the drag coefficient of the drops.

In the present study, the rate and distribution of impingement of waterdrops on a symmetrical, 15-percent-thick, Joukowski airfoil at angles of attack of 0° (Case I) and 2° (Case II) and on a cambered (a = 1 mean line), 15-percent-thick, Joukowski airfoil at 0° angle of attack (Case IV) are determined using a differential analyzer for solution of the differential equations and employing the experimentally determined drag coefficient of spheres to approximate the drag coefficient of the waterdrops. Figure 1 is a drawing of the three airfoil cases (Case III was to have been a study of the symmetrical, 15-percent-thick, Joukowski airfoil at 4° angle of attack, but it was decided to study Case IV in preference thereto.)

This project was under the general direction of L. M. K. Boelter. The authors wish to acknowledge the advice of John W. Hazen in the direction and implementation of the research program and the assistance of R. Peck and M. Potter in making the necessary computations for presentation of the data and also the assistance of the operators of the differential analyzer under E. Janssen and G. N. Brittle.

This work was conducted under the sponsorship and with the financial assistance of the National Advisory Committee for Aeronautics.

SYMBOLS

a	acceleration of drop, ft/sec^2
A	projected area of waterdrop, ft^2
C	chord length of airfoil, ft
C_D	drag coefficient of drop, [1]*
E	percentage catch based on maximum thickness of airfoil [1]
E_M	total percentage catch based on maximum thickness of airfoil [1]
f	drag force, #
m	mass of drop, lb or # sec^2/ft**
M	rate of impingement of waterdrops on a body, lb/hr ft span
P	velocity of drop relative to air, ft/sec
r	radius of drop, ft

* Dimensionless

** The abbreviation, lb, represents pound mass; the symbol, #, represents pound force.

R_P Reynolds Modulus for drop at relative velocity P, [1]

R_U Reynolds Modulus for drop at free-stream velocity, [1]

s position of impingement on surface of airfoil, measured from chord line, divided by chord length, [1]

S furthest position of impingement on surface of airfoil (i.e., trajectory tangent), measured from chord line, divided by chord length, [1]

t time, sec

u_a velocity component of air parallel to chord line, ft/sec

u_d velocity component of drop parallel to chord line, ft/sec

U free-stream velocity, ft/sec

v_a velocity component of air normal to chord line, ft/sec

v_d velocity component of drop normal to chord line, ft/sec

w liquid water content of cloud, lb/ft^3

x distance from the axis normal to chord line which intersects leading edge at chord line (i.e., distance from y-axis), divided by chord length, [1]

$\dot{x}_a$ $\frac{dx_a}{d\tau} = \frac{u_a}{U}$, [1]

$\dot{x}_d$ $\frac{dx_d}{d\tau} = \frac{u_d}{U}$, [1]

y distance from the axis parallel to chord line which intersects leading edge at chord line (i.e., distance from x-axis), divided by chord length, [1]

y_o distance of a trajectory from the x-axis at $x = -\infty$, divided by chord length, [1]

$\dot{y}_a$ $\frac{dy_a}{d\tau} = \frac{v_a}{U}$, [1]

$\dot{y}_d$ $\frac{dy_d}{d\tau} = \frac{v_d}{U}$, [1]

γ_a mass density of air, lb/ft^3

γ_d mass density of drop, lb/ft^3

μ absolute viscosity of air, lb/sec ft

ψ Scale Modulus, $9C\frac{\gamma_a}{r\gamma_d}$, [1]

τ Time Scale, $t\frac{U}{C}$, [1]

θ angle of relative velocity vector from x-axis [1]

α angle of attack of airfoil, deg

Subscripts:

A airfoil

C cylinder

L lower

U upper

1 first impinging trajectory

2 second impinging trajectory

ANALYSIS

In a cloud, the motion of a waterdrop which results when a body moves through that cloud with finite velocity is caused by the drag created by flow of the displaced air relative to the waterdrop. This resulting motion is the same as if the waterdrop had been suspended in air flowing over the stationary body with the same velocity. Making a force balance on the waterdrop (see fig. 2) one obtains:

$$\Sigma F = 0 = ma - f$$

$$\Sigma F_x = 0 = m\frac{du_d}{dt} - f\cos\theta \qquad (1)$$

$$\Sigma F_y = 0 = m\frac{dv_d}{dt} - f\sin\theta \qquad (2)$$

where f, the drag force, is:

$$f = \frac{C_D A\gamma_a P^2}{2} = \frac{C_D \pi r^2 \gamma_a P^2}{2}$$

and

$$\cos\theta = -\frac{(u_d - u_a)}{P} = \frac{u_a - u_d}{P}$$

$$\sin\theta = \frac{v_a - v_d}{P}$$

$$m = \frac{4}{3}\pi r^3 \gamma_d$$

Substituting in equations (1) and (2):

$$\frac{4}{3}\pi r^3 \gamma_d \frac{du_d}{dt} - \frac{C_D \pi r^2 \gamma_a P^2}{2} \frac{(u_a - u_d)}{P} = 0 \qquad (1a)$$

$$\frac{4}{3}\pi r^3 \gamma_d \frac{dv_d}{dt} - \frac{C_D \pi r^2 \gamma_a P^2}{2} \frac{(v_a - v_d)}{P} = 0 \qquad (2a)$$

These may be reduced to:

$$\frac{du_d}{dt} = \frac{3 C_D \gamma_a P}{8 r \gamma_d} (u_a - u_d) \qquad (3)$$

$$\frac{dv_d}{dt} = \frac{3 C_D \gamma_a P}{8 r \gamma_d} (v_a - v_d) \qquad (4)$$

Multiply both sides by $\frac{C}{U^2} \frac{3}{3} \frac{\mu}{2r} \frac{2r}{\mu} \frac{\gamma_a}{\gamma_a}$

$$\frac{d\left(\frac{(u_d)}{(U)}\right)}{d\left(\frac{(U_t)}{(C)}\right)} = \frac{(9C\gamma_a)}{(r\gamma_d)} \frac{(\mu)}{(2rU\gamma_a)} \frac{(C_D)}{(24)} \frac{(2rP\gamma_a)}{(\mu)} \frac{(u_a)}{(U)} - \frac{u_d)}{U)} \qquad (5)$$

$$\frac{d\left(\frac{(v_d)}{(U)}\right)}{d\left(\frac{(U)}{(C_t)}\right)} = \frac{(9C\gamma_a)}{(r\gamma_d)} \frac{(\mu)}{(2rU\gamma_a)} \frac{(C_D)}{(24)} \frac{(2rP\gamma_a)}{(\mu)} \frac{(v_a)}{(U)} - \frac{v_d)}{U)} \qquad (6)$$

Substituting in equations (5) and (6) the relationships:

$$\frac{u_d}{U} = \dot{x}_d, \quad t\frac{U}{C} = \tau, \quad \frac{9C\gamma_a}{r\gamma_d} = \Psi$$

$$\frac{u_a}{U} = \dot{x}_a, \quad \frac{v_d}{U} = \dot{y}_d, \quad \frac{v_a}{U} = \dot{y}_a$$

and

$$\frac{2rU\gamma_a}{\mu} = R_U, \quad \frac{2rP\gamma_a}{\mu} = R_P$$

gives

$$\frac{d\dot{x}_d}{d\tau} = \frac{\psi}{R_U}\frac{(C_D R_P)}{(24)}(\dot{x}_a - \dot{x}_d) \tag{7}$$

$$\frac{d\dot{y}_d}{d\tau} = \frac{\psi}{R_U}\frac{(C_D R_P)}{(24)}(\dot{y}_a - \dot{y}_d) \tag{8}$$

Equations (7) and (8) are the desired equations for the two-dimensional motion of a waterdrop in an air stream flowing over a body. For solution of the differential analyzer, these equations must be arranged as follows:

$$\dot{x}_d = \int (\dot{x}_a - \dot{x}_d)\, d\left\{\frac{\psi}{R_U}\int \frac{C_D R_P}{24}\, d\tau\right\}$$

$$\dot{y}_d = \int (\dot{y}_a - \dot{y}_d)\, d\left\{\frac{\psi}{R_U}\int \frac{C_D R_P}{24}\, d\tau\right\}$$

$$x = \int \dot{x}_d\, d\tau$$

$$y = \int \dot{y}_d\, d\tau$$

$$(\dot{x}_a - \dot{x}_d)^2 = \int 2(\dot{x}_a - \dot{x}_d)\, d(\dot{x}_a - \dot{x}_d)$$

$$(\dot{y}_a - \dot{y}_d)^2 = \int 2(\dot{y}_a - \dot{y}_d)d(\dot{y}_a - \dot{y}_d)$$

$$\left(\frac{P}{U}\right)^2 = (\dot{x}_a - \dot{x}_d)^2 + (\dot{y}_a - \dot{y}_d)^2$$

$$\frac{P}{U} = \int \frac{d(P/U)^2}{2(P/U)} \quad \text{(Inverse integrator)}$$

$$R_P = R_U \frac{P}{U}$$

$$\frac{C_D R_P}{24} = F_1(R_P) \qquad \text{Input table}$$

$$\dot{x}_a = F_2(x, y) \qquad \text{Input table}$$

$$\dot{y}_a = F_3(x, y) \qquad \text{Input table}$$

Knowledge of the magnitude of the quantities $\frac{C_D R_P}{24}$ (the ratio of the actual drag coefficient to the drag coefficient given by Stokes' law) and the velocity components of the air stream, $\dot{x}_a$ and $\dot{y}_a$, as a function of the location of the waterdrop relative to the body, must be available for the solution to proceed on the differential analyzer. The variation of $\frac{C_D R_P}{24}$ was taken from table I in reference 4. Plots of $\dot{x}_a$ and $\dot{y}_a$, the velocity components of the air stream, as functions of position relative to the airfoils under consideration were supplied by Ames Aeronautical Laboratory, Moffett Field, California.

Finally, having fixed ψ, the Scale Modulus (presented in reference 5), and R_U, the Reynolds Modulus of the drop based on free-stream velocity, solution of the equations can begin provided initial conditions for a trajectory are known. If it were possible to start the trajectory at infinite distance forward of the airfoil, there would be no question as to the initial conditions because the drop would have free-stream velocity at that distance. However, at a sufficiently large - though finite - distance ahead of the airfoil, the waterdrop still has essentially free-stream velocity. It is then necessary merely to determine this distance and start the trajectory there. (See section ESTABLISHMENT OF INITIAL CONDITIONS.)

As shown in figure 3, waterdrops started at different points will have different trajectories. A waterdrop which has its trajectory tangent to the upper surface of the airfoil will start at some

position $y = y_{o_U}$ when a large distance ahead of the airfoil. Another drop at some position $y = y_{o_L}$ when a large distance ahead of the airfoil will have a trajectory which is tangent to the lower surface of the airfoil. All drops located between y_{o_U} and y_{o_L} at this large distance ahead of the airfoil will have trajectories which intersect the airfoil surface, that is, the drops will impinge on the surface - specifically on that portion of the surface limited by the points of tangency of the tangent trajectories. All drops outside $y_{o_U} \geq y \geq y_{o_L}$ will miss the airfoil.

As mentioned previously, the area of impingement of waterdrops lies between the point of tangency on the upper surface and the point of tangency on the lower surface. Distribution over this area can be found by determining additional trajectories starting from points intermediate between y_{o_U} and y_{o_L}, such as y_{o_1} and y_{o_2} in figure 3.

The differential analyzer also gives the drop velocities at the points of impingement. This information is incidental to the immediate purpose of this study, but is included with the more pertinent material in this report for possible future use.

The more important assumptions which it has been necessary to make in arriving at the simplified problem which admits of solution are:

(1) At a large distance ahead of the airfoil, the drops move with free-stream velocity (that is, at the same velocity as the air) and with motion parallel to the free-stream path.

(2) The flow of air around the airfoil is that of an ideal fluid without turbulence or compressibility. (The drag of the air on the drop is that of a fluid having viscosity.)

(3) The drops are spherical.

(4) No gravitational force acts on the drop.

ESTABLISHMENT OF INITIAL CONDITIONS

In the study of waterdrop trajectories, the boundary conditions are that the waterdrops are traveling with free-stream velocity at $x = -\infty$ (that is, at infinite distance ahead of the airfoil). At finite distances from the leading edge of the airfoil, the drops have velocity components and positions varying between those given by the free stream and the streamlines.

For Airfoil Case I (shown at top in fig. 1), the divergence of the streamlines is 0.15 percent at $x = -3.05$, 0.3 percent at $x = -2.00$, and 1.2 percent at $x = -0.95$. Since the divergence is so small at $x = -3.05$ and even

at $x = -2.00$, postulating free-stream velocity and position for the drops at $x = -2.00$ should not cause great error in the trajectories. However, $x = -2.00$ is too great a distance for obtaining rapid results on the differential analyzer; $x = -0.95$ being about the maximum permissible approach to the airfoil leading edge (for a scale of 20 in. per chord length on the output table). It was determined on the analyzer that the assumption of free-stream values at $x = -2.00$, for small and intermediate values of $\Psi/R_U \left(2^{-3}, 2^0, 2^3\right)$, gave values of y and y_d at $x = -0.95$ which differed from the free-stream values by less than the expected precision of the analyzer, as seen in the following table:

	$\Psi/R_U = 2^{-3}$			$\Psi/R_U = 2^0$			$\Psi/R_U = 2^3$		
	$x = -2.0$ (Free-stream values)	$x = -0.95$	Diff.	$x = -2.0$ (Free-stream values)	$x = -0.95$	Diff.	$x = -2.0$ (Free-stream values)	$x = -0.95$	Diff.
y	0.07	0.07	0	0.0485	0.0486	-0.0001	0.015	0.015	0
$\dot{x}_d$	1.00	.9992	.0008	1.00	.9954	.0046	1.00	.9904	.0096
$\dot{y}_d$	0	0	0	0	.0001	-.0001	0	.0001	-.0001

The deviation of $\dot{x}_d$ from the free-stream value at $x = -0.95$ is not inappreciable but it was determined in the course of the investigation that the results obtained on the analyzer were the same regardless of whether $\dot{x}_d$ at $x = -0.95$ was chosen as the free-stream value or the streamline value.

Further, if choice of free-stream values at $x = -2.00$ gave values of y and $\dot{y}_d$ at $x = -0.95$ which were still very close to free-stream values, then choice of free-stream values at any x further from the airfoil than $x = -2.00$ would give free-stream values of y and $\dot{y}_d$ at $x = -2.00$ since the divergence in streamlines decreases as x becomes more negative and is already less than the expected precision of the analyzer at $x = -3.05$.

For large values of $\Psi/R_U\left(2^6\right)$, choice of streamline values for y and $\dot{y}_d$ at $x = -2.00$ resulted in obtaining values of y and $\dot{y}_d$ at $x = -0.95$ which differed from streamline values by less than the expected precision of the analyzer as shown in the following table.

$\psi/R_U = 2^6$				
	$x = -2.00$ (Streamline values)	$x = -0.95$ (Analyzer)	$x = -0.95$ (Streamline values)	Difference
y	0.002	0.002	0.002	0
$\dot{x}$	.997	.9883	.9882	.0001
$\dot{y}$	.00000	0	.0004	-.0004

Hence it would appear that for large values of ψ/R_U, the initial conditions should be streamline position and velocity components. However, for large values of ψ/R_U the positions of the drops whose trajectories are tangent to the upper and lower surfaces of the airfoil, respectively, are quite close together. At $x = -0.95$, the distance between the two positions (measured normal to the free-stream path) choosing streamline conditions differs by less than the expected precision of the analyzer from the distance obtained by choosing free-stream conditions.

On the basis of the above, free-stream values of drop position and velocity were taken as the initial conditions at $x = -0.95$ for all values of ψ/R_U considered.

For Airfoil Case II (shown at center in fig. 1), because of the effect of circulation, it was not possible to assume free-stream conditions at $x = -0.95$ for all cases, though the divergence of the streamlines was about 0.4 percent at $x = -2.0$ and about 1.4 percent at $x = -0.8$. Preliminary trajectories were run from $x = -0.8$ to the airfoil surface for various values of ψ/R_U using free-stream conditions as the initial conditions. For low values of ψ/R_U (2^{-3} and 2^{-6}) the choice of free-stream conditions as initial conditions seemed appropriate because the trajectories followed the path of the free stream for about 0.6 chord length before deviating appreciably and the y-component of velocity of the drop remained equal to the free-stream initial value for about the same distance. For higher values of ψ/R_U, the trajectories and y-component of velocity deviated from the free-stream values almost immediately, (about 0.1 chord length), indicating that free-stream conditions were not a suitable choice for initial conditions at $x = -0.8$.

For these larger values of ψ/R_U, the conditions at $x = -2.0$ were assumed to be free-stream conditions, and trajectories were run on the analyzer from $x = -2.0$ to $x = -0.8$ for various values of y_o and

for $\psi/R_U = 2^0$, 2^3, and 2^6. From these trajectories, the position and velocity components of a drop at $x = -0.8$ were determined as functions of ψ/R_U and of the position of the drop at $x = -2.0$. These data were then used as the starting conditions at $x = -0.8$ for the determination of the trajectories from $x = -0.8$ to the points of tangency or impingement on the airfoil surface.

Examination of the trajectories and y-component of velocity plots for $\psi/R_U = 2^0$, which were run from $x = -2.0$ to $x = -0.8$ using free-stream initial conditions, revealed that there was little deviation for about 0.3 chord length, an indication that choice of free-stream conditions as initial conditions at $x = -2.0$ was valid.

Choosing streamline conditions as initial conditions at $x = -2.0$ for $\psi/R_U = 2^6$ gave results which indicated that the waterdrops were still following the streamline at $x = -0.8$ ($\dot{x}_d = 0.9854$, $\dot{y}_d = 0.0558$; $\dot{x}_a = 0.9855$, $\dot{y}_a = 0.056$) and, consequently, that streamline conditions were probably more valid than free-stream conditions as initial conditions at $x = -2.0$. However for these large values of ψ/R_U, the "initial" positions of the drops whose trajectories are tangent to the upper and lower surfaces of the airfoil, respectively, are quite close together. At $x = -2.0$, the divergence of the streamlines is about 0.35 percent, on the average, (in the region of the trajectories) so postulating free-stream velocity and position as the initial conditions at $x = -2.0$ should not introduce too great an error even for the large values of ψ/R_U.

For Airfoil Case IV (shown at the bottom in fig. 1), the "working" initial conditions, that is, those to be used when starting the drop trajectories at $x = -0.8$, were determined by making preliminary runs from $x = -2.0$ to $x = -0.8$, (as was done for Case II) assuming the drops to have free-stream velocity and position at $x = -2.0$. From these runs, the position and velcoity components of the drop at $x = -0.8$ were determined as functions of y_o, the starting position at $x = -2.0$. The y-positions of the drops relative to one another at $x = -2.0$ are the same as at $x = -\infty$ under the assumption that the drops have free-stream velocity and position at $x = -2.0$. The validity of this assumption for most values of ψ/R_U was substantiated, as for Case II, by examination of the trajectories for the runs from $x = -2.0$ to $x = -0.8$. Again, for $2^{-6} < \psi/R_U < 2^6$, the trajectories followed the free-stream path for about 0.3 chord length before beginning to deviate and the y-components of the drop velocity did not change from the free-stream value (0) given them initially over approximately the same distance. For higher values of ψ/R_U, the choice of streamline conditions as initial conditions seemed more valid because the trajectories obtained followed the streamlines even at $x = -0.8$. However, for the same reasons given for Case II, free-stream initial conditions were assumed even at high values of ψ/R_U.

RESULTS

The differential-analyzer solutions of the equations of motion of the waterdrops were in the form of plots of the y-position of the waterdrop as a function of x and the x-component and y-component of velocity of the waterdrop as a function of x, the distance ahead of the airfoil leading edge. The y versus x plots were drawn on an output table with a scale drawing of the particular airfoil mounted at one side of the table to establish the x and y frame of reference. (See fig. 3.) In obtaining the tangent trajectory, the analyzer was operated such that a trial trajectory, started at some initial y-position, y_o, was drawn up to the vicinity of the airfoil surface. If the trajectory missed the airfoil surface or impinged at some point short of the point of tangency, a new estimate of the initial y-position of the tangent trajectory was made and a second trajectory run on the analyzer. This trajectory was usually close enough to the tangent one to permit interpolation (or extrapolation), though occasionally (in the first runs for any airfoil) one or two more trials might be necessary to determine the tangent trajectory satisfactorily. Supplementary trajectories, with initial y_o values intermediate between the values for the trajectories tangent to the upper and lower surfaces of the airfoil, were run to their points of impingement on the airfoil to permit determination of the distribution of the impingement.

The rate of impingement of water on that portion of the surface of a body bounded by the point of tangency (S_L) on the lower surface and the point of tangency (S_U) on the upper surface, is (per unit span):

$$M_A = \Delta y_o U w$$

$$= \left(y_{o_U} - y_{o_L}\right) U w \tag{9}$$

where $\Delta y_o \left(= y_{o_U} - y_{o_L}\right)$ is the distance between the initial positions of the upper and lower tangent trajectories, U is the free-stream velocity, and w is the liquid water content of the cloud.

Equation (9) may be rewritten in terms of an efficiency of water catch, E_M, and the maximum catch based on the maximum thickness of the airfoil (that is, the catch of the airfoil when the waterdrop trajectories are along the free-stream path), then

$$M_A = U w E_M \text{ (Maximum thickness)} \tag{10}$$

and

$$E_M = \frac{y_{o_U} - y_{o_L}}{\text{Maximum thickness}} \tag{11}$$

For the intermediate trajectories (see fig. 3), the rate of impingement of water on that portion of the surface of the body bounded by the point of tangency (S_L) on the lower surface and the point of impingement of the intermediate trajectory (1) is

$$M_{A_1} = UwE \text{ (Maximum thickness)} \tag{12}$$

where

$$E = E_M \frac{y_{o_1} - y_{o_L}}{y_{o_U} - y_{o_L}}$$

y_{o_1} being the initial position of the intermediate trajectory.

From equations (10) and (12)

$$\frac{M_{A_1}}{M_A} = \frac{E}{E_M}$$

These equations are the defining equations for the quantities (E_M, E/E_M) which are plotted as functions of R_U and ψ and which, with the plots of s_U and s_L versus R_U, ψ, permit the computation of the rate and distribution of impingement of waterdrops on a particular airfoil, given the necessary data to calculate R_U and ψ.

Tables I, II, and III are summaries of the data obtained using the differential analyzer for Airfoil Case I, Airfoil Case II, and Airfoil Case IV, respectively. The values of $\dot{x}_d$ and $\dot{y}_d$ are the drop velocities at the points of impingement or tangency. This information is incidental to the immediate purpose of this study, but is included with the more pertinent material because of the possible need for it at some future time. These values of $\dot{x}_d$ and $\dot{y}_d$ are reliable except at high values of ψ/R_U when the velocity components of the drop change rapidly near the nose of the airfoil.

Figures 4, 9, and 18 are plots of E_M, the total percentage catch versus the Scale Modulus, ψ, with the Reynolds Modulus, R_U, as parameter, for Airfoil Cases I, II, and IV, respectively. At low values of ψ, the curves of constant R_U approach a value of E_M which is the maximum attainable for the particular airfoil case. This maximum value of E_M is equal to the ratio of the projected frontal thickness of the airfoil to the maximum thickness of the airfoil (15 percent chord in each Airfoil Case). The values of y_o upon which the E_M values are based are estimated to be good to 0.0001, as far as the precision of the differential analyzer is concerned. Since E_M is essentially the difference between

two values of y_o, at worst the error is about 0.0002. For values of $E_M \cong 100$ percent, the percentage error is about 0.2 percent but for values of $E_M \cong 10$ percent and lower, the percentage error is 2 percent and higher. Hence, at very high values of ψ/R_U ($\psi/R_U = 2^6$) when there may be some question of the validity of free-stream conditions as initial conditions at $x = -2.0$, the precision of the differential analyzer is such that even if the correct initial conditions had been used, the percentage error would still have been at least 2 percent or higher.

The precision of the trajectories could be increased by enlarging the scale, but then consideration must be made of the running time for each trajectory on the differential analyzer. The question of the scale necessary to give the desired precision while not causing the running time per trajectory to be excessive is one which is posed whether the integration be performed numerically or on any kind of computer.

Figure 5 is a plot of S_U, the distance along the upper airfoil surface to the point of tangency of the tangent trajectory (that is, the furthest point of impingement on the upper surface of the airfoil), as a function of ψ with R_U as parameter for Case I. S_L, the distance along the lower airfoil surface to the point of tangency of the tangent trajectory (that is, the furthest point of impingement on the lower surface of the airfoil), is equal in magnitude to S_U because the airfoil is symmetrical and at $\alpha = 0^\circ$, for Case I. All curves of constant R_U approach the value $S_U(= S_L) = 0.283$, the point on the surface at which the airfoil has its maximum thickness, as ψ decreases (waterdrops increase in diameter). For Case I, there can be no impingement beyond this point on either surface.

Figures 10 and 11 are plots of S_U and S_L versus ψ and R_U for Case II. The maximum value of S_U is now 0.241 and that for S_L is 0.321. These values correspond to the case when $\psi/R_U = 0$ (that is, when there is no deflection of the drop by the streamlines).

Figures 19 and 20 are similar plots for Case IV. The maximum value of S_U is 0.325 and that for S_L is 0.220. As before, these values correspond to the case when there is no deflection of the drop by the streamlines ($\psi/R_U = 0$).

The data plotted in figures 5, 10, 11, 19, and 20 were obtained by scaling off the distances to the points of tangency on the output plots of the differential analyzer. The location of the exact point of tangency was not accurately determinable because of the thickness of the ink-line representing the trajectory and because of the large radius of curvature of both the trajectory and also of the airfoil surface when the trajectory is tangent in the region aft of the nose of the airfoil. The precision of location of the points of tangency is estimated to be such as to give

a "maximum error" of about ±0.002 (in terms of chord) at the lower ends of the curves, ±0.005 (in terms of chord) at the center, and ±0.015 (in terms of chord) at the upper ends of the curves. This maximum error is not a measure of any inherent error in the analyzer trajectory, but is only a measure of the indeterminacy of the location of the point tangency. The lowest and highest estimations of the location of this point were used in determining the magnitude of the maximum error and it is probable that the actual error was much less than the maximum.

Figures 6 and 7, 12 to 14, and 21 to 23 are plots of E/E_M versus s, the distance along the airfoil surface (in terms of chord length) for various values of ψ/R_U with R_U as parameter, for Case I, Case II, and Case IV, respectively. The quantity E/E_M is the ratio of the percentage catch between the point of tangency on the lower surface and any point of impingement on the airfoil to the total percentage catch between the point of tangency on the lower surface and point of tangency on the upper surface.

Figures 8, 15 to 17, and 24 to 26 are replots of the data of the preceding paragraph, ψ/R_U now being the variable parameter and R_U being the fixed parameter. In the former figures, variation of R_U with ψ/R_U constant did not affect the distribution greatly (except at high values of ψ/R_U) but variation of ψ/R_U with R_U constant changes the distribution greatly for all values of R_U, as shown in these latter figures. The dashed curve for $\psi/R_U = 2^{-\infty}(\psi/R_U = 0)$ drawn in figures 15 to 17 and 24 to 26 is based on computed values and is a limiting distribution which is obtained when the drops are not deflected by the streamlines (that is, when the drops are very large). This dashed curve is not drawn in figure 8 because it almost coincides with the curve drawn for $\psi/R_U = 2^{-6}$.

DISCUSSION OF RESULTS

As can be seen from reference 5, the total percentage catch, E_M, the area of impingement per foot of span, $S_U - S_L$, and the distribution of impingement, E/E_M, are functions of ψ, the Scale Modulus, and R_U, the Reynolds Modulus. The range of ψ and R_U used in these studies encompasses most combinations of the following range of variables:

Variable	Maximum value	Minimum value
2r	100	20 microns
U	400	100 mph
γ_a	(sea level) 2.378×10^{-3}	(20,000 ft) 1.267×10^{-3} lb sec^2/ft^4
μ	3.75×10^{-7}	3.4×10^{-7} lb sec/ft^2
C	30.0	0.25 ft
γ_d	1.94	1.94 lb sec^2/ft^4

Figures 4, 9, and 18, which are plots of E_M versus ψ with R_U as parameter for Case I, Case II, and Case IV, respectively, show that E_M, based on the maximum thickness of the airfoil, becomes greater than 100 percent when the projected frontal thickness of the airfoil becomes greater than the maximum thickness of the airfoil, as it does for Case II and Case IV. The shape of the curves of constant R_U is the same, in general, but the slopes tend to differ at the upper and lower ends. The five values of the parameter R_U for Case I bracket the four values for Case II and Case IV. The reduction in number of values was desirable because the number of runs was correspondingly reduced while the range of variables was still encompassed, for the most part. In order to be able to compare figure 4 directly with figures 9 and 18, the dashed lines for the intermediate values of R_U were obtained by interpolation.

Comparison of figure 5 with figures 10 and 11 shows that at an angle of attack of 2°, the symmetrical 15-percent-thick Joukowski airfoil exhibits points of tangency of the tangent trajectories which are closer to the leading edge on the upper surface and further from the leading edge on the lower surface than for the same airfoil at angle of attack of 0°, as was to be expected. Also, comparison of the distribution curves in figures 6 to 8 with those shown in figures 12 to 18 shows that the curves in the latter are not symmetrical about the point $s = 0$ and, consequently, that some 60 to 80 percent of the total catch impinges on the lower surface of the airfoil instead of the catch being distributed evenly between upper and lower surfaces.

Inspection of the distribution curves for Case IV (figs. 21 to 23 or figs. 24 to 26) shows that from 50 to 60 percent of the total catch impinges on the upper surface of the cambered airfoil except when the drops are small and the velocity (R_U) very high. In this instance, about 60 percent of the catch is on the lower surface of the cambered airfoil.

In general, the distribution curves for all three airfoil cases show that for a given value of ψ/R_U the effect of varying R_U is not too great but that for a given value of R_U the effect of varying ψ/R_U is quite great, that is, drop size is relatively more important than velocity in determining the distribution of catch.

Figures 27 to 29 show comparisons of the rate of water impingement for the respective airfoils to the rate of water impingement on two cylinders; one with a diameter equal to twice the radius of the leading edge of the airfoil, the other with a diameter equal to the maximum thickness of the airfoil (15 percent chord). The comparisons are made for a low and a high value of R_U. At high values of ψ the former comparison is somewhat better, whereas at low values of ψ, the latter comparison is much better. This was to be expected because large waterdrops (ψ low) are not deflected greatly by the air flow and the catch per foot span is dependent only on the projected frontal thickness which is the same in the latter instance previously mentioned.

CONCLUSIONS

1. The rates of water impingement on the three airfoil cases studied cannot be determined satisfactorily by assuming these rates to be equal to the rates of water impingement on cylinders except for limited ranges of ψ, the Scale Modulus. However, they can be determined within ±25 percent for values of ψ between 1 and about 100 or 10,000 (depending upon the value of R_U), by assuming the rates to be equal to the rates of water impingement on a cylinder whose radius is equal to the maximum thickness of the airfoil.

2. With respect to distribution, the effect of drop size is greater than the effect of velocity.

3. Increase of angle of attack of a symmetrical 15-percent-thick, Joukowski airfoil from $\alpha = 0^\circ$ to $\alpha = 2^\circ$, or change from a symmetrical 15-percent-thick, Joukowski, to a cambered, a = 1 mean line, 15-percent-thick, Joukowski airfoil, does not change the rate of water impingement greatly (especially at low ψ and high R_U) but does change the area of impingement and the distribution of impingement to a greater extent.

Department of Engineering
University of California
Los Angeles 24, Calif., October 5, 1948

REFERENCES

1. Glauert, Muriel: A Method of Constructing the Paths of Raindrops of Different Diameters Moving in the Neighbourhood of (1) A Circular Cylinder, (2) an Aerofoil, Placed in a Uniform Stream of Air; and a Determination of the Rate of Deposit of the Drops on the Surface and the Percentage of Drops Caught. R. & M. No. 2025, British A. R. C., 1940.

2. Kantrowitz, Arthur: Aerodynamic Heating and the Deflection of Drops by an Obstacle in an Air Stream in Relation to Aircraft Icing. NACA TN No. 779, 1940.

3. Bergrun, Norman R.: A Method for Numerically Calculating the Area and Distribution of Water Impingement on the Leading Edge of an Airfoil in a Cloud. NACA TN No. 1397, 1947.

4. Langmuir, Irving, and Blodgett, Katherine B.: A Mathematical Investigation of Water Droplet Trajectories. General Electric Co. Rep., 1945. (Also available as Army Air Forces Tech. Rep. No. 5418 and as Dept. of Commerce Pub. PB No. 27565.)

5. Boelter, L. M. K., Young, George, and Tribus, Myron: The Limitations and Mathematical Basis for Predicting Aircraft Icing Characteristics from Scale Model Studies. Section V of Army Air Forces Tech. Rep. No. 5529, Nov. 6, 1946, pp. 63-78.

TABLE I

WATERDROP TRAJECTORY VALUES OBTAINED FROM DIFFERENTIAL ANALYZER FOR JOUKOWSKI AIRFOIL,

Symmetrical 15% Thick $\alpha = 0^\circ$

Date	Run No.	ψ	R_U	y_o	Surface	s	$\frac{1}{d}$	$\frac{1}{d}$	$y_o - y_{o_L}$	$\frac{E}{E_M} = \frac{y_o - y_{o_L}}{y_{o_U} - y_{o_L}}$	$\frac{E_M}{100} = \frac{(y_{o_U} - y_{o_L})\cos\alpha}{\text{Max Thickness}}$
4/27/48	1-1-3-1	2^1	2^7	0.074	Upper*	0.265	1.0	0	0.148	1.0	0.987
4/27/48	1-1-3-1	2^1	2^7	-0.074	Lower*	-0.265	1.0	0	0	0	
4/22/48	1-1-4-2	2^3	2^9	0.074	Upper*	0.273	0.997	0.004	0.148	1.0	0.987
4/22/48	1-1-4-2	2^3	2^9	-0.074	Lower*	-0.273	0.997	-0.004	0	0	
4/22/48	1-1-5-3	2^5	2^{11}	0.072	Upper*	0.262	0.997	0.013	0.144	1.0	0.960
4/22/48	1-1-5-3	2^5	2^{11}	-0.072	Lower*	-0.262	0.997	-0.013	0	0	
4/27/48	1-2-2-1	2^2	2^5	0.073	Upper*	0.273	1.0	0.012	0.146	1.0	0.973
4/27/48	1-2-2-1	2^2	2^5	-0.073	Lower*	-0.273	1.0	-0.012	0	0	
4/22/48	1-2-3-1	2^4	2^7	0.070	Upper*	0.244	1.005	0.023	0.140	1.0	0.933
4/22/48	1-2-3-12	2^4	2^7	0.045	Upper	0.068	0.99	0.013	0.115	0.821	
4/22/48	1-2-3-11	2^4	2^7	0.020	Upper	0.021	0.982	0.009	0.090	0.643	
4/22/48	1-2-3-11	2^4	2^7	-0.020	Lower	-0.021	0.982	-0.009	0.050	0.357	
4/22/48	1-2-3-12	2^4	2^7	-0.045	Lower	-0.068	0.99	-0.013	0.025	0.178	
4/22/48	1-2-3-1	2^4	2^7	-0.070	Lower*	-0.244	1.005	-0.023	0	0	
4/23/48	1-2-4-2	2^6	2^9	0.0655	Upper*	0.225	1.004	0.043	0.131	1.0	0.873
4/23/48	1-2-4-2	2^6	2^9	-0.0655	Lower*	-0.225	1.004	-0.043	0	0	
4/23/48	1-2-5-2	2^8	2^{11}	0.058	Upper*	0.188	1.007	0.092	0.116	1.0	0.773
4/23/48	RR 1-2-5-22	2^8	2^{11}	0.040	Upper	0.058	0.949	0.069	0.098	0.845	
4/23/48	1-2-5-21	2^8	2^{11}	0.020	Upper	0.023	0.931	0.029	0.078	0.672	
4/23/48	1-2-5-21	2^8	2^{11}	-0.020	Lower	-0.023	0.931	-0.029	0.038	0.328	
4/23/48	RR 1-2-5-22	2^8	2^{11}	-0.040	Lower	-0.058	0.949	-0.069	0.018	0.155	
4/23/48	1-2-5-2	2^8	2^{11}	-0.058	Lower*	-0.188	1.007	-0.092	0	0	
4/27/48	RR 1-3-1-3	2^3	2^3	0.059	Upper*	0.197	0.994	0.078	0.118	1.0	0.787
4/27/48	RR 1-3-1-3	2^3	2^3	-0.059	Lower*	-0.197	0.994	-0.078	0	0	
4/26/48	1-3-2-3	2^5	2^5	0.056	Upper*	0.185	0.992	0.089	0.112	1.0	0.747
4/26/48	1-3-2-3	2^5	2^5	-0.056	Lower*	-0.185	0.992	-0.089	0	0	
5/3/48	RR 1-3-3-3	2^7	2^7	0.0485	Upper*	0.150	0.989	0.149	0.097	1.0	0.647
5/3/48	RR 1-3-3-3	2^7	2^7	-0.0485	Lower*	-0.150	0.989	-0.149	0	0	
4/26/48	1-3-4-2	2^9	2^9	0.038	Upper*	0.108	0.941	0.225	0.076	1.0	0.507
4/26/48	1-3-4-2	2^9	2^9	-0.038	Lower*	-0.108	0.941	-0.225	0	0	
4/26/48	1-3-5-2	2^{11}	2^{11}	0.025	Upper*	0.072	0.856	0.349	0.050	1.0	0.333
4/26/48	1-3-5-2	2^{11}	2^{11}	-0.025	Lower*	-0.072	0.856	-0.349	0	0	

*Tangent Trajectory.

NACA

TABLE I - Concluded

WATERDROP TRAJECTORY VALUES OBTAINED FROM DIFFERENTIAL ANALYZER FOR JOUKOWSKI AIRFOIL,

Symmetrical 15% Thick $\alpha = 0°$

Date	Run No.	ψ	R_U	y_o	Surface	s	$\dot{x}_d$	$\dot{y}_d$	$y_o - y_{o_L}$	$\frac{E}{E_M} = \frac{y_o - y_{o_L}}{y_{o_U} - y_{o_L}}$	$\frac{E_M}{100} = \frac{(y_{o_U} - y_{o_L}) \cos \alpha}{\text{Max. Thickness}}$
4/30/48	RR 1-4-1-3	2^6	2^3	0.0255	Upper*	0.078	0.870	0.321	0.0510	1.0	0.340
4/21/48	1-4-1-22	2^6	2^3	0.018	Upper	0.031	0.693	0.192	0.0435	0.853	
4/21/48	1-4-1-21	2^6	2^3	0.008	Upper	0.010	0.698	0.061	0.0335	0.657	
4/21/48	1-4-1-21	2^6	2^3	-0.008	Lower	-0.010	0.698	-0.061	0.0175	0.343	
4/21/48	1-4-1-22	2^6	2^3	-0.018	Lower	-0.031	0.693	-0.192	0.0075	0.147	
4/30/48	RR 1-4-1-3	2^6	2^3	-0.0255	Lower*	-0.078	0.870	-0.321	0	0	
5/3/48	RR_2 1-4-2-1	2^8	2^5	0.021	Upper*	0.073	0.828	0.359	0.042	1.0	0.280
5/3/48	RR_2 1-4-2-1	2^8	2^5	-0.021	Lower*	-0.073	0.828	-0.359	0	0	
4/21/48	1-4-3-3	2^{10}	2^7	0.0145	Upper*	0.050	0.681	0.476	0.0290	1.0	0.193
4/21/48	1-4-3-32	2^{10}	2^7	0.0100	Upper	0.020	0.572	0.198	0.0245	0.845	
4/21/48	1-4-3-31	2^{10}	2^7	0.0050	Upper	0.009	0.563	0.109	0.0195	0.672	
4/21/48	1-4-3-31	2^{10}	2^7	-0.0050	Lower	-0.009	0.563	-0.109	0.0095	0.328	
4/21/48	1-4-3-32	2^{10}	2^7	-0.0100	Lower	-0.020	0.572	-0.198	0.0045	0.155	
4/21/48	1-4-3-3	2^{10}	2^7	-0.0145	Lower*	-0.050	0.681	-0.476	0	0	
4/30/48	RR_2 1-4-3-3	2^{10}	2^7	0.0150	Upper*	0.052	0.741	0.451	0.030	1.0	0.200
4/30/48	RR_2 1-4-3-3	2^{10}	2^7	-0.0150	Lower*	-0.052	0.741	-0.451	0	0	
5/5/48	RR_3 1-4-3-2	2^{10}	2^7	0.0165 -0.0165	Upper* Lower*	----- -----	----- -----	----- -----	0.0330 0	1.0 0	0.220
4/27/48	1-4-4-3	2^{12}	2^9	0.0110	Upper*	0.038	0.584	0.452	0.022	1.0	0.147
4/27/48	1-4-4-3	2^{12}	2^9	-0.0110	Lower*	-0.038	0.584	-0.452	0	0	
5/4/48	RR 1-4-4-1	2^{12}	2^9	0.0090 -0.0090	Upper* Lower*	----- -----	----- -----	----- -----	0.0180 0	1.0 0	0.120
4/27/48	1-4-5-2	2^{14}	2^{11}	0.0040	Upper*	0.022	0.329	0.469	0.0080	1.0	0.053
4/27/48	1-4-5-2	2^{14}	2^{11}	-0.0040	Lower*	-0.022	0.329	-0.469	0	0	
4/26/48	1-5-1-6	2^9	2^3	0.0040	Upper*	0.029	0.430	0.466	0.0080	1.0	0.053
4/26/48	1-5-1-6	2^9	2^3	-0.0040	Lower*	-0.029	0.430	-0.466	0	0	
5/5/48	RR 1-5-1-3	2^9	2^3	0.0035	Upper*	0.023	0.355	0.514	0.0070	1.0	0.047
5/5/48	RR 1-5-1-3	2^9	2^3	-0.0035	Lower*	-0.023	0.355	-0.514	0	0	
4/26/48	1-5-3-1	2^{13}	2^7	0.0025	Upper*	0.025	0.401	0.451	0.0050	1.0	0.033
4/26/48	1-5-3-1	2^{13}	2^7	-0.0025	Lower*	-0.025	0.401	-0.451	0	0	
5/5/48	RR 1-5-3-2	2^{13}	2^7	0.0020	Upper*	0.015	0.251	0.401	0.0040	1.0	0.027
5/5/48	RR 1-5-3-2	2^{13}	2^7	-0.0020	Lower*	-0.015	0.251	-0.401	0	0	
5/5/48	RR 1-5-4-1	2^{15}	2^9	0.0005 -0.0005	Upper* Lower*	0.016 -0.016	0.187 0.187	0.459 -0.459	0.0010 0	1.0 0	0.007

*Tangent Trajectory.

NACA

TABLE II

WATERDROP TRAJECTORY VALUES OBTAINED FROM DIFFERENTIAL ANALYZER FOR JOUKOWSKI AIRFOIL,

Symmetrical 15% Thick $\alpha = 2^\circ$

Date	Run No.	Ψ	R_U	y_o	Surface	s	x_d	y_d	$y_o - y_{o_L}$	$\frac{E}{E_M} = \frac{y_o - y_{o_L}}{y_{o_U} - y_{o_L}}$	$\frac{E_M}{100} = \frac{(y_{o_U} - y_{o_L})\cos\alpha}{\text{Max. Thickness}}$
6/23/48	2-1-3-2U	2^2	2^8	-0.0046	Upper*	0.236	1.001	0.041	0.1502	1.000	1.001
6/23/48	2-1-3-2L	2^2	2^8	-0.1548	Lower*	-0.316	0.998	0.035	0.0000	0.000	
6/24/48	2-1-4-2U	2^4	2^{10}	-0.0055	Upper*	0.223	1.003	0.044	0.1484	1.000	0.989
6/24/48	2-1-4-2L	2^4	2^{10}	-0.1539	Lower*	-0.310	0.998	0.030	0.0000	0.000	
6/24/48	2-2-1-3U	2^1	2^4	-0.0081	Upper*	0.226	1.009	0.053	0.1452	1.000	0.967
6/24/48	2-2-1-3L	2^1	2^4	-0.1533	Lower*	-0.311	0.997	0.027	0.0000	0.000	
6/24/48	2-2-2-3U	2^3	2^6	-0.0095	Upper*	0.212	1.011	0.062	0.1437	1.000	0.957
6/24/48	2-2-2-1D	2^3	2^6	-0.0381	Upper	0.045	0.983	0.054	0.1156	0.805	
6/24/48	2-2-2-2D	2^3	2^6	-0.0667	Upper	0.005	0.984	0.044	0.0870	0.605	
6/24/48	2-2-2-3D	2^3	2^6	-0.0956	Lower	-0.026	0.974	0.039	0.0581	0.405	
6/24/48	2-2-2-4D	2^3	2^6	-0.1243	Lower	-0.082	0.972	0.033	0.0294	0.205	
6/24/48	2-2-2-2L	2^3	2^6	-0.1532	Lower*	-0.308	0.997	0.022	0.0000	0.000	
6/25/48	2-2-3-1U	2^5	2^8	-0.0140	Upper*	0.196	1.015	0.083	0.1368	1.000	0.911
6/25/48	2-2-3-1D	2^5	2^8	-0.0410	Upper	0.041	0.980	0.066	0.1098	0.802	
6/25/48	2-2-3-2D	2^5	2^8	-0.0683	Upper	0.003	0.969	0.052	0.0825	0.602	
6/25/48	2-2-3-3D	2^5	2^8	-0.0958	Lower	-0.026	0.970	0.038	0.0550	0.402	
6/25/48	2-2-3-4D	2^5	2^8	-0.1232	Lower	-0.078	0.975	0.024	0.0276	0.202	
6/25/48	2-2-3-2L	2^5	2^8	-0.1508	Lower*	-0.295	0.995	0.013	0.0000	0.000	
6/28/48	2-2-4-2U	2^7	2^{10}	-0.0214	Upper*	0.168	1.021	0.126	0.1274	1.000	0.849
6/28/48	2-2-4-1D	2^7	2^{10}	-0.0464	Upper	0.034	0.958	0.100	0.1022	0.802	
6/28/48	2-2-4-2D	2^7	2^{10}	-0.0721	Upper	0.002	0.941	0.063	0.0767	0.601	
6/28/48	2-2-4-3D	2^7	2^{10}	-0.0977	Lower	-0.027	0.939	0.032	0.0511	0.401	
6/28/48	2-2-4-4D	2^7	2^{10}	-0.1231	Lower	-0.079	0.955	0.004	0.0257	0.202	
6/28/48	2-2-4-3L	2^7	2^{10}	-0.1488	Lower*	-0.265	0.992	-0.008	0.0000	0.000	
6/28/48	2-3-1-2U	2^4	2^4	-0.0435	Upper*	0.149	1.010	0.160	0.1163	1.000	0.775
6/28/48	2-3-1-3L	2^4	2^4	-0.1598	Lower*	-0.245	0.984	-0.023	0.0000	0.000	
6/28/48	2-3-2-3U	2^6	2^6	-0.0493	Upper*	0.128	1.012	0.202	0.1065	1.000	0.710
6/28/48	2-3-2-1D	2^6	2^6	-0.0705	Upper	0.027	0.908	0.140	0.0853	0.800	
6/28/48	2-3-2-2D	2^6	2^6	-0.0902	Lower	-0.001	0.881	0.083	0.0638	0.598	
6/28/48	2-3-2-3D	2^6	2^6	-0.1130	Lower	-0.027	0.881	0.033	0.0428	0.402	
6/28/48	2-3-2-4D	2^6	2^6	-0.1345	Lower	-0.071	0.921	-0.013	0.0213	0.200	
6/28/48	2-3-2-3L	2^6	2^6	-0.1558	Lower*	-0.225	0.983	-0.052	0.0000	0.000	
6/29/48	2-3-3-3U	2^8	2^8	-0.0587	Upper*	0.100	0.999	0.283	0.0888	1.000	0.592
6/29/48	2-3-3-1D	2^8	2^8	-0.0763	Upper	0.022	0.852	0.189	0.0712	0.801	
6/29/48	2-3-3-2D	2^8	2^8	-0.0940	Lower	-0.002	0.827	0.103	0.0535	0.603	
6/29/48	2-3-3-3D	2^8	2^8	-0.1118	Lower	-0.023	0.815	0.015	0.0357	0.402	
6/29/48	2-3-3-4D	2^8	2^8	-0.1298	Lower	-0.058	0.863	-0.050	0.0177	0.199	
6/29/48	2-3-3-2L	2^8	2^8	-0.1475	Lower*	-0.177	0.963	-0.105	0.0000	0.000	

*Tangent Trajectory.

TABLE II -- Concluded

WATERDROP TRAJECTORY VALUES OBTAINED FROM DIFFERENTIAL ANALYZER FOR JOUKOWSKI AIRFOIL,

Symmetrical 15% Thick $\alpha = 2^\circ$

Date	Run No.	Ψ	R_U	y_o	Surface	s	$\dot{x}_d$	$\dot{y}_d$	$y_o - y_{o_L}$	$\frac{E}{E_M} = \frac{y_o - y_{o_L}}{y_{o_U} - y_{o_L}}$	$\frac{E_M}{100} = \frac{(y_{o_U} - y_{o_L})\cos\alpha}{\text{Max. Thickness}}$
6/30/48	2-3-4-2U	2^{10}	2^{10}	-0.0743	Upper*	0.063	0.914	0.424	0.0617	1.000	0.411
6/30/48	2-3-4-2L	2^{10}	2^{10}	-0.1360	Lower*	-0.118	0.902	-0.195	0.0000	0.000	
6/30/48	2-4-1-3U	2^{7}	2^{4}	-0.0955	Upper*	0.055	0.881	0.472	0.0475	1.000	0.317
6/30/48	2-4-1-1D	2^{7}	2^{4}	-0.1065	Upper	0.009	0.758	0.250	0.0365	0.768	
6/30/48	2-4-1-2D	2^{7}	2^{4}	-0.1160	Lower	-0.004	0.637	0.113	0.0270	0.569	
6/30/48	2-4-1-3D	2^{7}	2^{4}	-0.1250	Lower	-0.017	0.642	-0.006	0.0180	0.379	
6/30/48	2-4-1-4D	2^{7}	2^{4}	-0.1335	Lower	-0.036	0.685	-0.109	0.0095	0.200	
6/30/48	2-4-1-4L	2^{7}	2^{4}	-0.1430	Lower*	-0.098	0.854	-0.246	0.0000	0.000	
7/1/48	2-4-2-2U	2^{9}	2^{6}	-0.1005	Upper*	0.038	0.767	0.528	0.0377	1.000	0.251
7/1/48	2-4-2-1D	2^{9}	2^{6}	-0.1080	Upper	0.009	0.553	0.303	0.0297	0.802	
7/1/48	2-4-2-2D	2^{9}	2^{6}	-0.1155	Lower	-0.004	0.542	0.132	0.0232	0.603	
7/1/48	2-4-2-3D	2^{9}	2^{6}	-0.1230	Lower	-0.016	0.535	-0.011	0.0152	0.403	
7/1/48	2-4-2-4D	2^{9}	2^{6}	-0.1310	Lower	-0.034	0.611	-0.235	0.0072	0.191	
7/1/48	2-4-2-2L	2^{9}	2^{6}	-0.1382	Lower*	-0.079	0.813	0.300	0.0000	0.000	
7/1/48	2-4-3-3U	2^{11}	2^{8}	-0.1085	Upper*	0.024	0.562	0.611	0.0240	1.000	0.160
7/1/48	2-4-3-1D	2^{11}	2^{8}	-0.1130	Upper	0.004	0.394	0.255	0.0195	0.813	
7/1/48	2-4-3-2D	2^{11}	2^{8}	-0.1182	Lower	-0.005	0.379	0.118	0.0143	0.596	
7/1/48	2-4-3-3D	2^{11}	2^{8}	-0.1228	Lower	-0.014	0.377	-0.061	0.0097	0.404	
7/1/48	2-4-3-4D	2^{11}	2^{8}	-0.1275	Lower	-0.029	0.498	-0.186	0.0050	0.208	
7/1/48	2-4-3-4L	2^{11}	2^{8}	-0.1325	Lower*	-0.055	0.688	-0.356	0.0000	0.000	
7/2/48	2-4-4-3U	2^{13}	2^{10}	-0.1165	Upper*	0.010	0.210	0.514	0.0110	1.000	0.073
7/2/48	2-4-4-1D	2^{13}	2^{10}	-0.1190	Upper	0.000	0.357	0.230	0.0085	0.772	
7/2/48	2-4-4-2D	2^{13}	2^{10}	-0.1218	Lower	-0.004	0.300	0.130	0.0057	0.473	
7/2/48	2-4-4-3D	2^{13}	2^{10}	-0.1250	Lower	-0.012	0.273	-0.072	0.0025	0.227	
7/2/48	2-4-4-3L	2^{13}	2^{10}	-0.1275	Lower*	-0.033	0.444	-0.399	0.0000	0.000	
7/6/48	2-5-1-5U	2^{10}	2^{4}	-0.1232	Upper*	0.008	0.186	0.610	0.0030	1.000	0.020
7/6/48	2-5-1-5L	2^{10}	2^{4}	-0.1262	Lower*	-0.015	0.100	-0.243	0.0000	0.000	
7/7/48	2-5-2-3U	2^{12}	2^{6}	-0.1243	Upper*	0.003	0.090	0.434	0.0035	1.000	0.023
7/7/48	2-5-2-3L	2^{12}	2^{6}	-0.1278	Lower*	-0.015	0.246	-0.235	0.0000	0.000	
7/7/48	2-5-3-4U	2^{14}	2^{8}	-0.1254	Upper*	0.002	0.103	0.506	0.0021	1.000	0.014
7/7/48	2-5-3-4L	2^{14}	2^{8}	-0.1275	Lower*	-0.014	0.175	-0.295	0.0000	0.000	

*Tangent Trajectory.

TABLE III

WATERDROP TRAJECTORY VALUES OBTAINED FROM DIFFERENTIAL ANALYZER FOR JOUKOWSKI AIRFOIL,

Cambered $a = 1$ Mean Line — 15% Thick — $\alpha = 6^\circ$

Date	Run No.	ψ	B_U	y_o	Surface	s	$\dot{x}_d$	$\dot{y}_d$	$y_o - y_{o_L}$	$\frac{E}{E_M} = \frac{y_o - y_{o_L}}{y_{o_U} - y_{o_L}}$	$\frac{E_M}{100} = \frac{(y_{o_U} - y_{o_L}) \cos \alpha}{\text{Max. thickness}}$
7/12/48	4-1-3-3U	2^2	2^8	0.0935	Upper*	0.317	1.003	0.007	0.1500	1.000	1.000
7/12/48	4-1-3-2L	2^2	2^8	-0.0565	Lower*	-0.216	0.998	-0.002	0.0000	0.000	
7/12/48	4-1-4-2U	2^4	2^{10}	0.0915	Upper*	0.310	1.006	0.013	0.1480	1.000	0.987
7/12/48	4-1-4-2L	2^4	2^{10}	-0.0565	Lower*	-0.213	0.999	-0.006	0.0000	0.000	
7/12/48	4-2-1-4U	2^1	2^4	0.0855	Upper*	0.305	1.009	0.022	0.1455	1.000	0.970
7/12/48	4-2-1-4L	2^1	2^4	-0.0600	Lower*	-0.215	0.994	-0.001	0.0000	0.000	
7/12/48	4-2-2-3U	2^3	2^6	0.0818	Upper*	0.294	1.012	0.031	0.1428	1.000	0.952
7/12/48	4-2-2-1D	2^3	2^6	0.0536	Upper	0.096	0.992	0.022	0.1146	0.802	
7/12/48	4-2-2-2D	2^3	2^6	0.0253	Upper	0.038	0.988	0.020	0.0863	0.604	
7/12/48	4-2-2-3D	2^3	2^6	-0.0038	Upper	0.002	0.985	0.011	0.0572	0.401	
7/12/48	4-2-2-4D	2^3	2^6	-0.0318	Lower	-0.033	0.984	0.003	0.0292	0.204	
7/12/48	4-2-2-2L	2^3	2^6	-0.0610	Lower*	-0.212	0.999	-0.008	0.0000	0.000	
7/13/48	4-2-3-2U	2^5	2^8	0.0775	Upper*	0.275	1.022	0.050	0.1375	1.000	0.917
7/13/48	4-2-3-1D	2^5	2^8	0.0503	Upper	0.092	0.989	0.042	0.1103	0.802	
7/13/48	4-2-3-2D	2^5	2^8	0.0225	Upper	0.034	0.976	0.030	0.0825	0.600	
7/13/48	4-2-3-3D	2^5	2^8	-0.0045	Upper	0.001	0.972	0.017	0.0555	0.404	
7/13/48	4-2-3-4D	2^5	2^8	-0.0325	Lower	-0.033	0.973	0.002	0.0275	0.200	
7/13/48	4-2-3-2L	2^5	2^8	-0.0600	Lower*	-0.199	0.990	-0.016	0.0000	0.000	
7/13/48	4-2-4-2U	2^7	2^{10}	0.0660	Upper*	0.243	1.033	0.090	0.1245	1.000	0.830
7/13/48	4-2-4-1D	2^7	2^{10}	0.0420	Upper	0.077	0.976	0.075	0.1005	0.807	
7/13/48	4-2-4-2D	2^7	2^{10}	0.0160	Upper	0.030	0.954	0.054	0.0745	0.598	
7/13/48	4-2-4-3D	2^7	2^{10}	-0.0085	Upper	0.000	0.943	0.024	0.0500	0.402	
7/13/48	4-2-4-4D	2^7	2^{10}	-0.0335	Lower	-0.032	0.946	-0.006	0.0250	0.201	
7/13/48	4-2-4-2L	2^7	2^{10}	-0.0585	Lower*	-0.183	0.984	-0.036	0.0000	0.000	
7/14/48	4-3-1-4U	2^4	2^4	0.0377	Upper*	0.211	1.028	0.128	0.1147	1.000	0.765
7/14/48	4-3-1-3L	2^4	2^4	-0.0770	Lower*	-0.180	0.978	-0.042	0.0000	0.000	
7/14/48	4-3-2-2U	2^6	2^6	0.0312	Upper*	0.192	1.038	0.168	0.1043	1.000	0.695
7/14/48	4-3-2-1D	2^6	2^6	0.0100	Upper	0.061	0.936	0.131	0.0831	0.797	
7/14/48	4-3-2-2D	2^6	2^6	-0.0110	Upper	0.022	0.898	0.095	0.0621	0.595	
7/14/48	4-3-2-3D	2^6	2^6	-0.0315	Lower	-0.003	0.884	0.048	0.0416	0.399	
7/14/48	4-3-2-4D	2^6	2^6	-0.0525	Lower	-0.031	0.891	-0.007	0.0206	0.198	
7/14/48	4-3-2-2L	2^6	2^6	-0.0731	Lower*	-0.157	0.971	-0.073	0.0000	0.000	
7/15/48	4-3-3-2U	2^8	2^8	0.0180	Upper*	0.158	1.038	0.238	0.0860	1.000	0.573
7/15/48	4-3-3-1D	2^8	2^8	0.0010	Upper	0.050	0.893	0.188	0.0690	0.802	
7/15/48	4-3-3-2D	2^8	2^8	-0.0165	Upper	0.018	0.839	0.127	0.0515	0.599	
7/15/48	4-3-3-3D	2^8	2^8	-0.0340	Lower	-0.004	0.820	0.054	0.0340	0.395	
7/15/48	4-3-3-4D	2^8	2^8	-0.0510	Lower	-0.028	0.838	-0.017	0.0170	0.198	
7/15/48	4-3-3-2L	2^8	2^8	-0.0680	Lower*	-0.120	0.940	-0.129	0.0000	0.000	

*Tangent Trajectory.

NACA

TABLE III - Concluded

WATERDROP TRAJECTORY VALUES OBTAINED FROM DIFFERENTIAL ANALYZER FOR JOUKOWSKI AIRFOIL,

Cambered a = 1 Mean Line 15% Thick $\alpha = 0^\circ$

Date	Run No.	ψ	R_U	y_o	Surface	s	x_d	y_d	$y_o - y_{o_L}$	$\frac{E}{E_M} = \frac{y_o - y_{o_L}}{y_{o_U} - y_{o_L}}$	$\frac{E_M}{100} = \frac{(y_{o_U} - y_{o_L})\cos\alpha}{\text{Max. Thickness}}$
7/15/48	4-3-4-2U	2^{10}	2^{10}	0.0000	Upper*	0.109	1.000	0.357	0.0620	1.000	0.413
7/15/48	4-3-4-2L	2^{10}	2^{10}	-0.0620	Lower*	-0.085	0.883	-0.220	0.0000	0.000	
7/15/48	4-4-1-3U	2^{7}	2^{4}	-0.0280	Upper*	0.092	0.958	0.405	0.0492	1.000	0.328
7/15/48	4-4-1-1D	27	2^{4}	-0.0382	Upper	0.032	0.727	0.288	0.0390	0.793	
7/15/48	4-4-1-2D	27	2^{4}	-0.0480	Upper	0.012	0.638	0.189	0.0292	0.593	
7/15/48	4-4-1-3D	27	2^{4}	-0.0575	Lower	-0.004	0.649	0.060	0.0197	0.400	
7/15/48	4-4-1-4D	27	2^{4}	-0.0670	Lower	-0.019	0.644	-0.046	0.0102	0.207	
7/15/48	4-4-1-5L	27	2^{4}	-0.0772	Lower*	-0.068	0.838	-0.264	0.0000	0.000	
7/16/48	4-4-2-3U	2^{9}	2^{6}	-0.0347	Upper*	0.072	0.911	0.487	0.0378	1.000	0.252
7/16/48	4-4-2-1D	2^{9}	2^{6}	-0.0425	Upper	0.025	0.634	0.350	0.0300	0.794	
7/16/48	4-4-2-2D	2^{9}	2^{6}	-0.0500	Upper	0.010	0.535	0.208	0.0225	0.595	
7/16/48	4-4-2-3D	2^{9}	2^{6}	-0.0582	Lower	-0.005	0.485	0.031	0.0143	0.378	
7/16/48	4-4-2-4D	2^{9}	2^{6}	-0.0660	Lower	-0.018	0.544	-0.124	0.0065	0.172	
7/16/48	4-4-2-3L	2^{9}	2^{6}	-0.0725	Lower*	-0.053	0.754	-0.319	0.0000	0.000	
7/16/48	4-4-3-4U	2^{11}	2^{8}	-0.0440	Upper*	0.046	0.686	0.576	0.0245	1.000	0.163
7/19/48	4-4-3-1D	2^{11}	2^{8}	-0.0500	Upper	0.015	0.448	0.360	0.0185	0.755	
7/19/48	4-4-3-2D	2^{11}	2^{8}	-0.0548	Upper	0.005	0.381	0.192	0.0137	0.559	
7/19/48	4-4-3-3D	2^{11}	2^{8}	-0.0594	Lower	-0.004	0.368	0.048	0.0091	0.371	
7/19/48	4-4-3-4D	2^{11}	2^{8}	-0.0638	Lower	-0.013	0.407	-0.103	0.0050	0.204	
7/16/48	4-4-3-4L	2^{11}	2^{8}	-0.0685	Lower*	-0.038	0.604	-0.384	0.0000	0.000	
7/19/48	4-4-4-4U	2^{13}	2^{10}	-0.0548	Upper*	0.025	0.471	0.650	0.0102	1.000	0.068
7/19/48	4-4-4-1D	2^{13}	2^{10}	-0.0569	Upper	0.007	0.258	0.308	0.0081	0.794	
7/19/48	4-4-4-2D	2^{13}	2^{10}	-0.0590	Lower	-0.001	0.178	0.082	0.0060	0.588	
7/19/48	4-4-4-3D	2^{13}	2^{10}	-0.0610	Lower	-0.008	0.184	-0.079	0.0040	0.392	
7/19/48	4-4-4-4D	2^{13}	2^{10}	-0.0630	Lower	-0.012	0.211	-0.168	0.0020	0.196	
7/19/48	4-4-4-2L	2^{13}	2^{10}	-0.0650	Lower*	-0.025	0.464	-0.428	0.0000	0.000	
7/20/48	4-5-1-3U	2^{10}	2^{4}	-0.0604	Upper	0.022	0.346	0.561	0.0096	1.000	0.064
7/20/48	4-5-1-4L	2^{10}	2^{4}	-0.0700	Lower	-0.018	0.317	-0.368	0.0000	0.000	
7/21/48	4-5-2-4U	2^{12}	2^{6}	-0.0650	Upper	0.015	0.285	0.527	0.0025	1.000	0.017
7/21/48	4-5-2-2L	2^{12}	2^{6}	-0.0675	Lower	-0.012	0.143	-0.253	0.0000	0.000	
7/21/48	4-5-3-2U	2^{14}	2^{8}	-0.0655	Upper	0.006	0.113	0.391	0.0015	1.000	0.010
7/21/48	4-5-3-1L	2^{14}	2^{8}	-0.0670	Lower	-0.008	0.046	-0.118	0.0000	0.000	

*Tangent Trajectory.

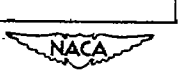

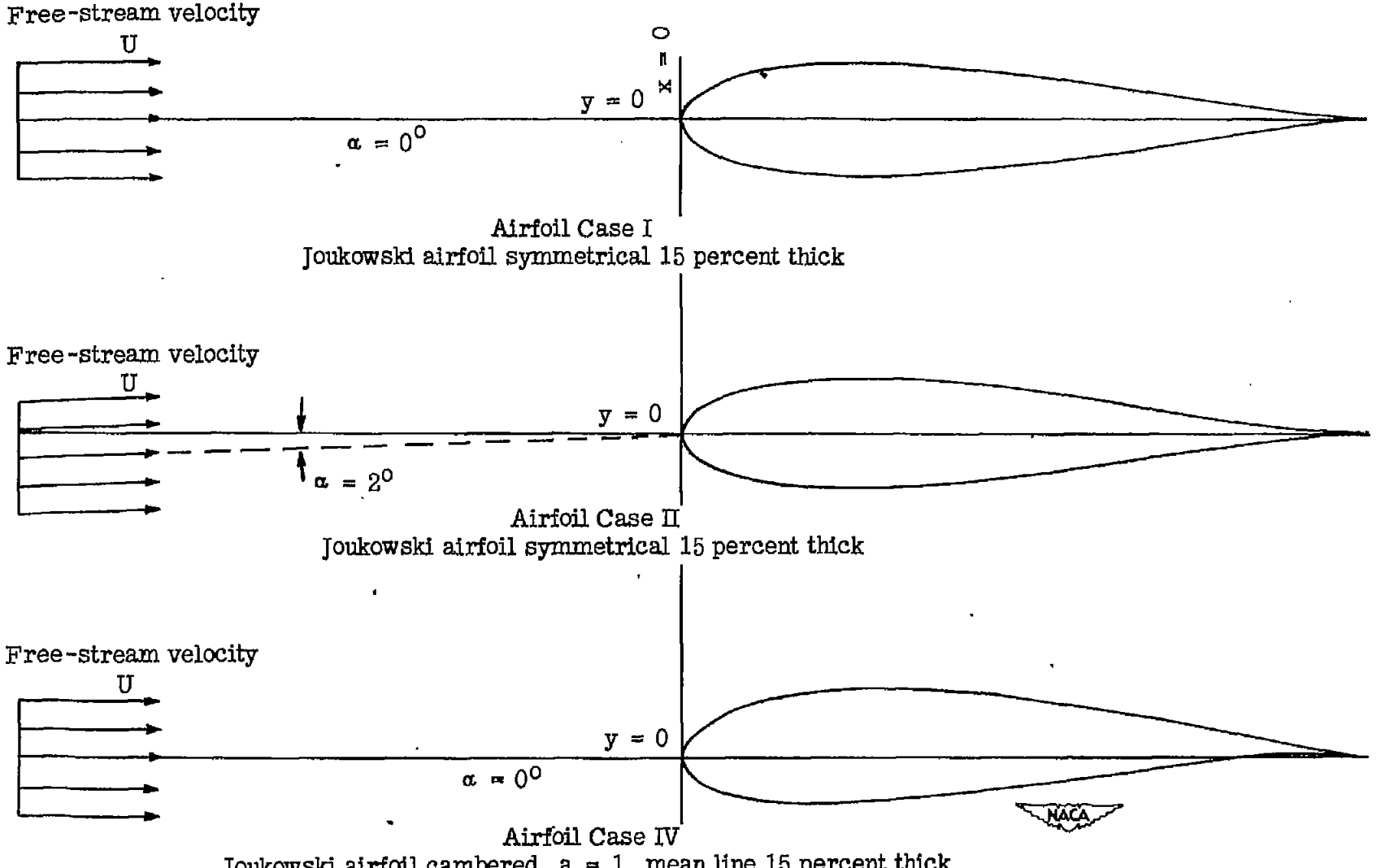

Figure 1.- Drawing of three airfoil - angle-of-attack combinations.

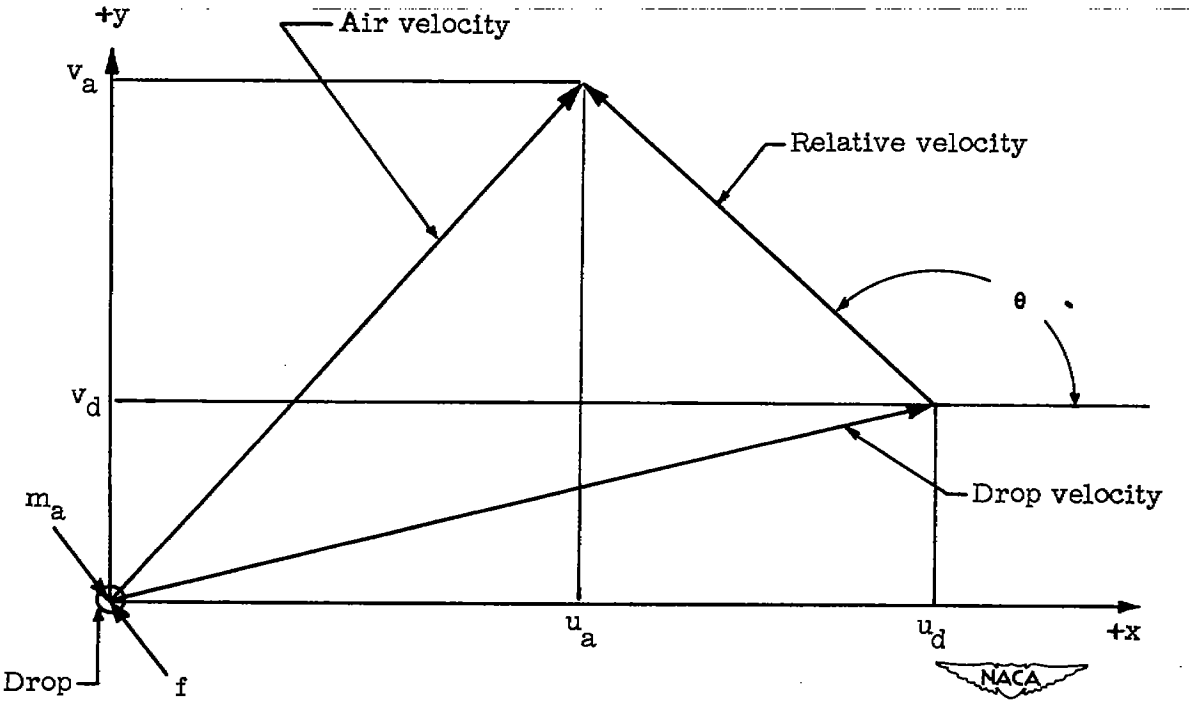

Figure 2.- Diagram of velocity components of air stream and waterdrop.

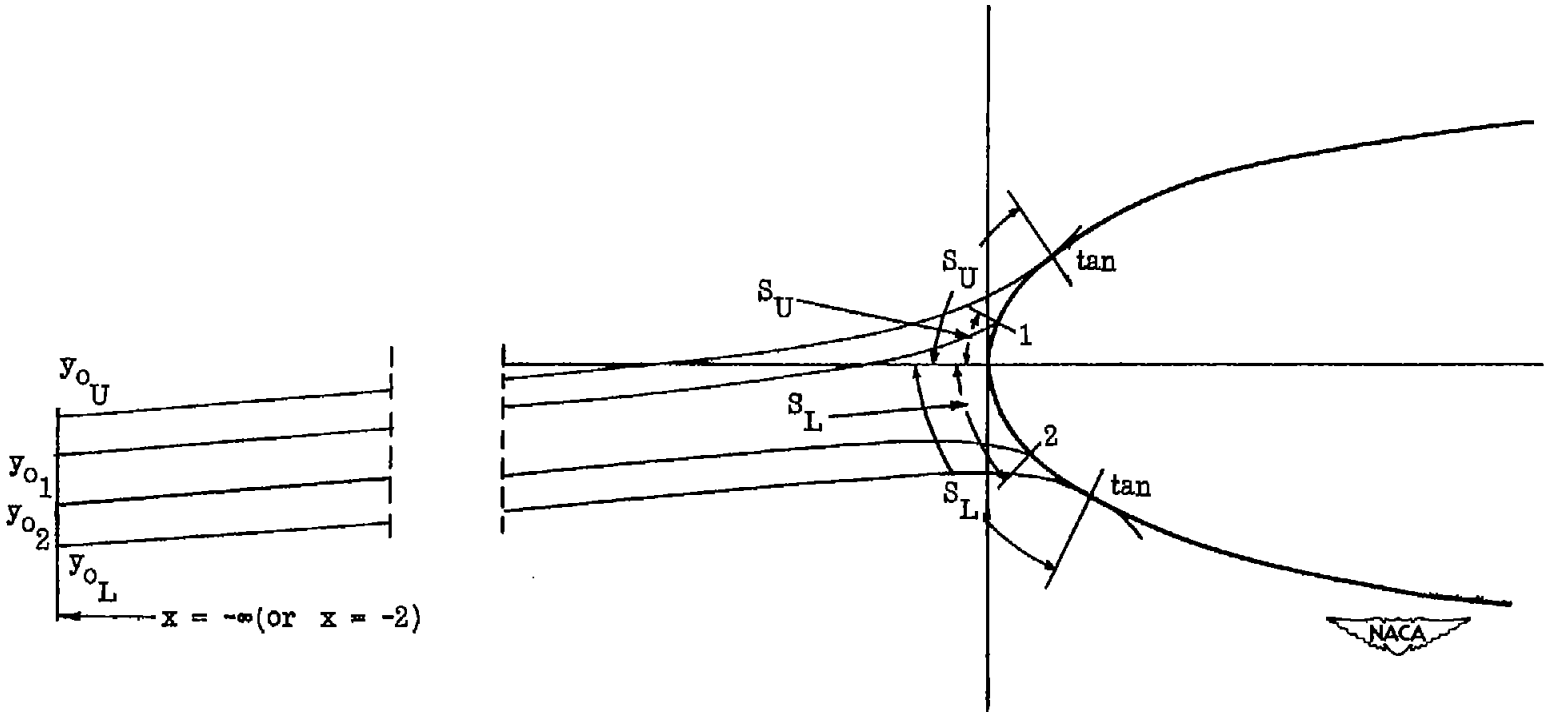

Figure 3.- Typical data taken from output plots of the differential analyzer.

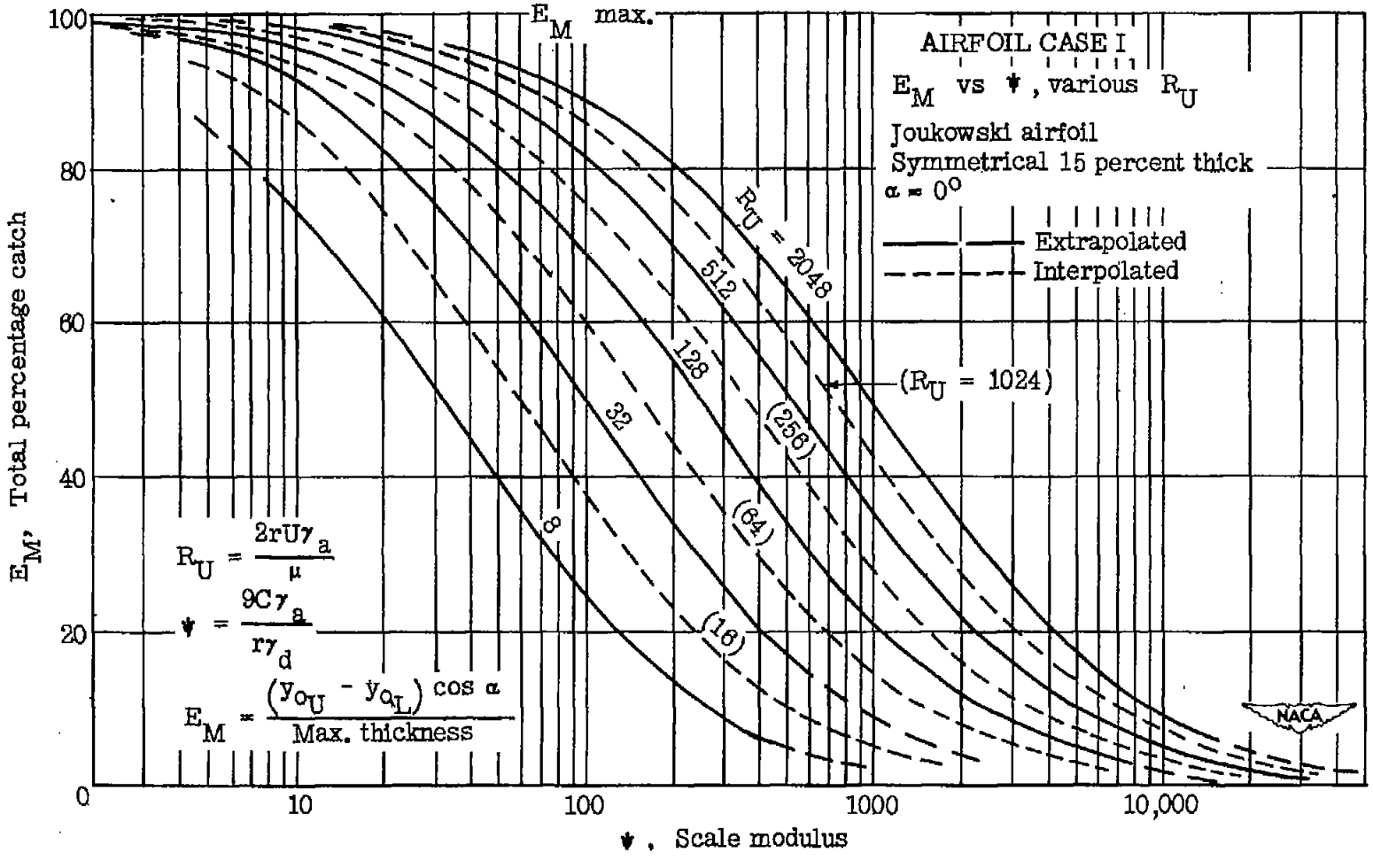
E_M max.
AIRFOIL CASE I
E_M vs Ψ, various R_U
Joukowski airfoil
Symmetrical 15 percent thick
$\alpha = 0^\circ$
Extrapolated
Interpolated
R_U = 2048
512
128
32
8
(256)
(64)
(16)
(R_U = 1024)
$R_U = \frac{2rU\gamma_a}{\mu}$
$\Psi = \frac{9C\gamma_a}{r\gamma_d}$
$E_M = \frac{(y_{o_U} - y_{o_L}) \cos \alpha}{\text{Max. thickness}}$
E_M, Total percentage catch
Ψ, Scale modulus
100
80
60
40
20
0
10
100
1000
10,000
NACA

Figure 4.

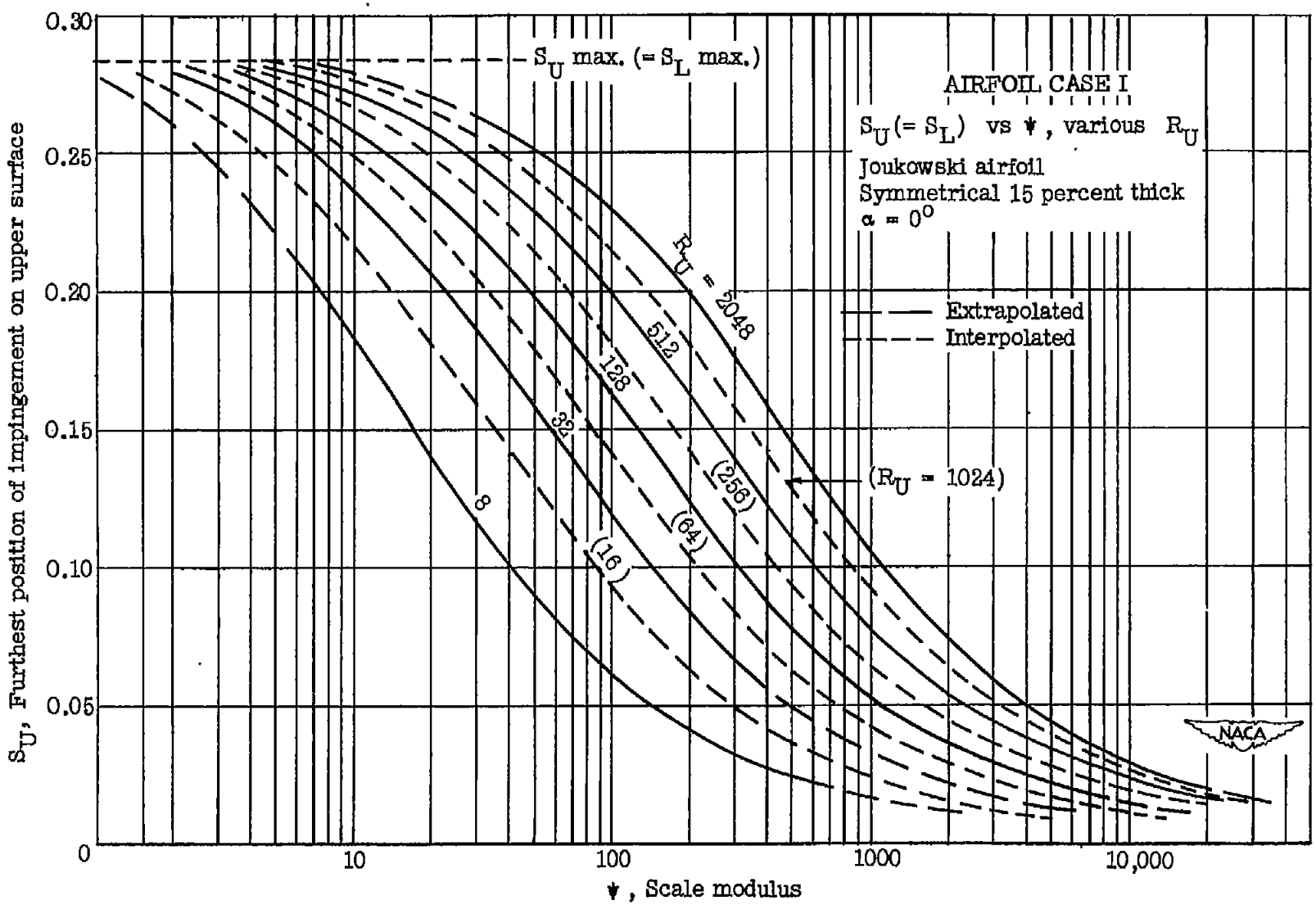
AIRFOIL CASE I
$S_U(= S_L)$ vs Ψ, various R_U
Joukowski airfoil
Symmetrical 15 percent thick
$\alpha = 0^\circ$
Extrapolated
Interpolated
S_U max. ($= S_L$ max.)
R_U = 2048
512
128
32
8
(256)
(64)
(16)
(R_U = 1024)
NACA
0.30
0.25
0.20
0.15
0.10
0.05
0
10
100
1000
10,000
S_U, Furthest position of impingement on upper surface
Ψ, Scale modulus

Figure 5.

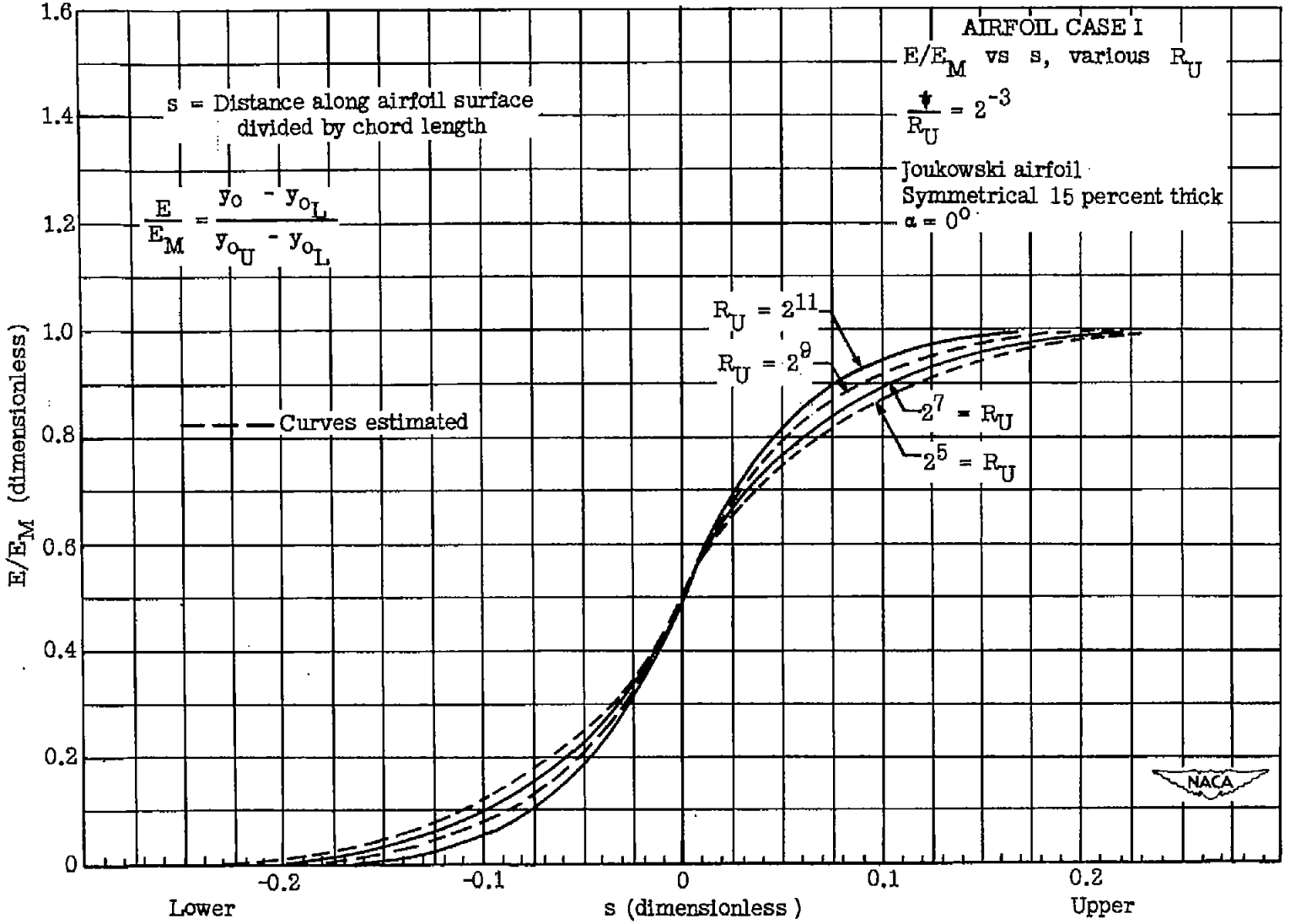
AIRFOIL CASE I
E/E_M vs s, various R_U
t/R_U = 2^-3
Joukowski airfoil
Symmetrical 15 percent thick
α = 0°
s = Distance along airfoil surface divided by chord length
E/E_M = (y_o - y_oL) / (y_oU - y_oL)
R_U = 2^11
R_U = 2^9
2^7 = R_U
2^5 = R_U
Curves estimated
NACA
E/E_M (dimensionless)
s (dimensionless)
Lower
Upper
1.6
1.4
1.2
1.0
0.8
0.6
0.4
0.2
0
-0.2
-0.1
0
0.1
0.2

Figure 6.

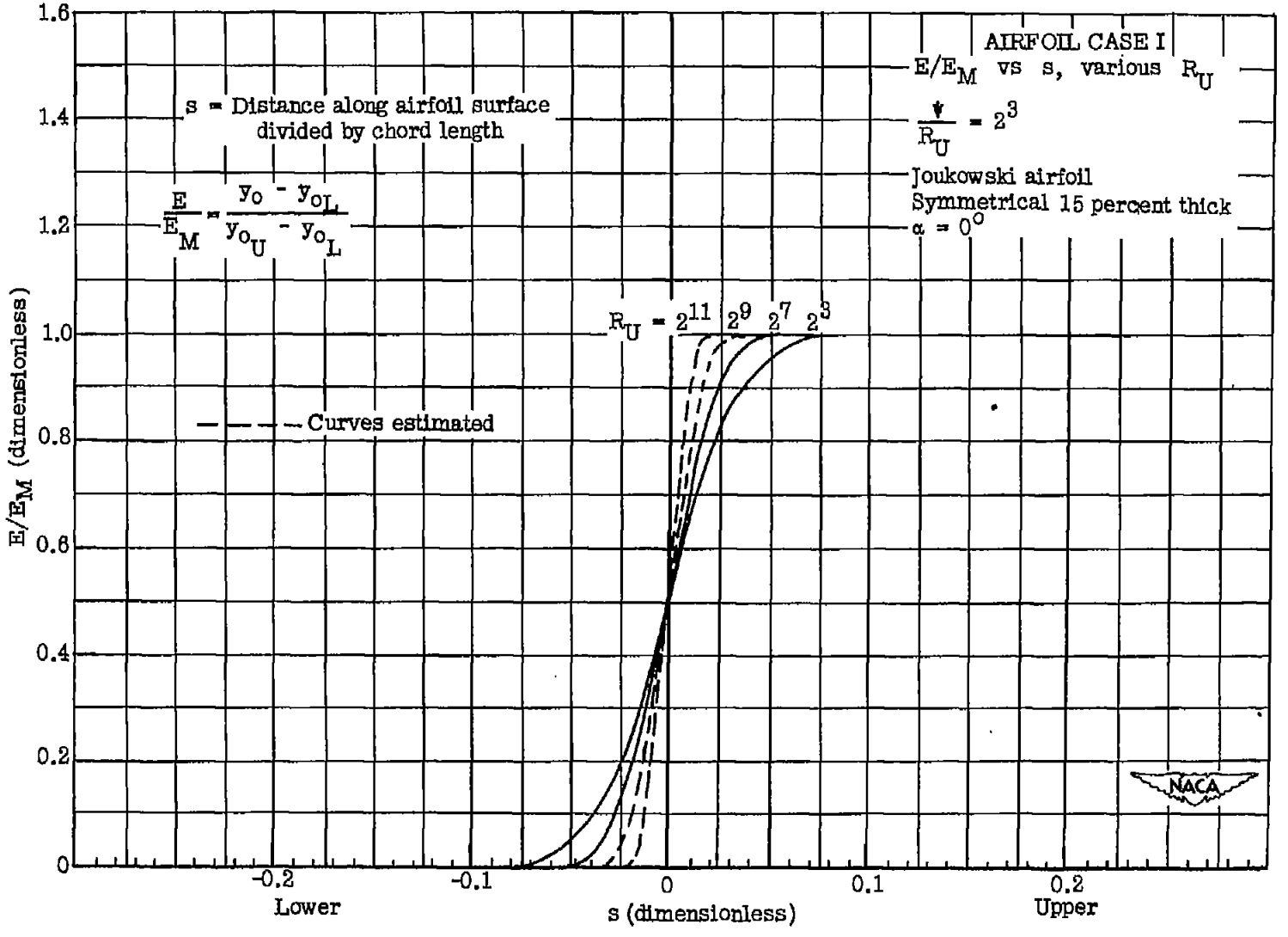
AIRFOIL CASE I
E/E_M vs s, various R_U
t/R_U = 2^3
Joukowski airfoil
Symmetrical 15 percent thick
α = 0°
s = Distance along airfoil surface divided by chord length
E/E_M = (y_o - y_oL) / (y_oU - y_oL)
R_U = 2^11 2^9 2^7 2^3
Curves estimated
E/E_M (dimensionless)
s (dimensionless)
Lower
Upper
NACA

Figure 7.

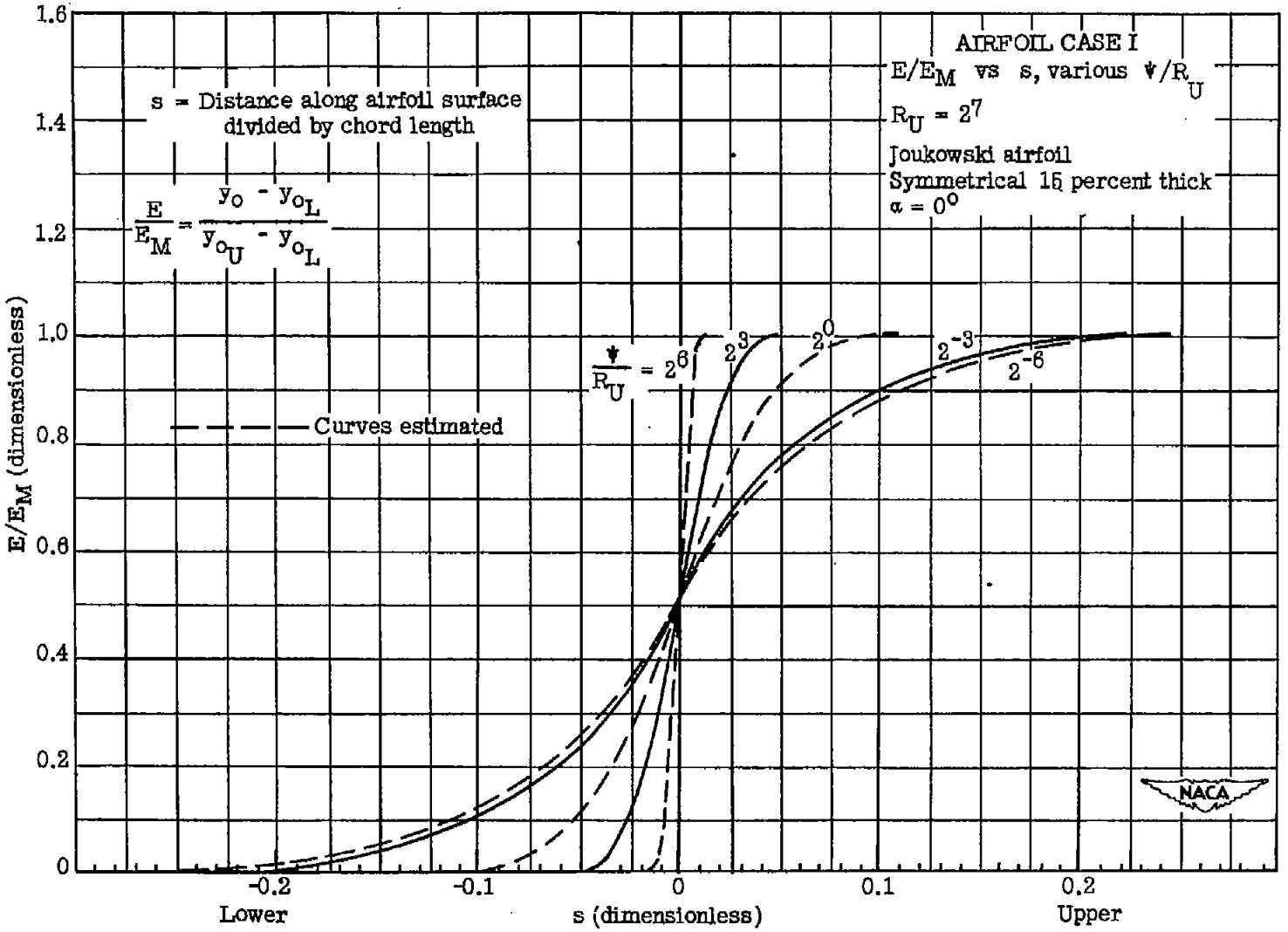
AIRFOIL CASE I
E/E_M vs s, various ψ/R_U
R_U = 2^7
Joukowski airfoil
Symmetrical 15 percent thick
α = 0°
s = Distance along airfoil surface divided by chord length
E/E_M = (y_o - y_oL) / (y_oU - y_oL)
ψ/R_U = 2^6 2^3 2^0 2^-3 2^-6
Curves estimated
NACA
E/E_M (dimensionless)
1.6
1.4
1.2
1.0
0.8
0.6
0.4
0.2
0
-0.2
-0.1
0
0.1
0.2
Lower
s (dimensionless)
Upper

Figure 8.

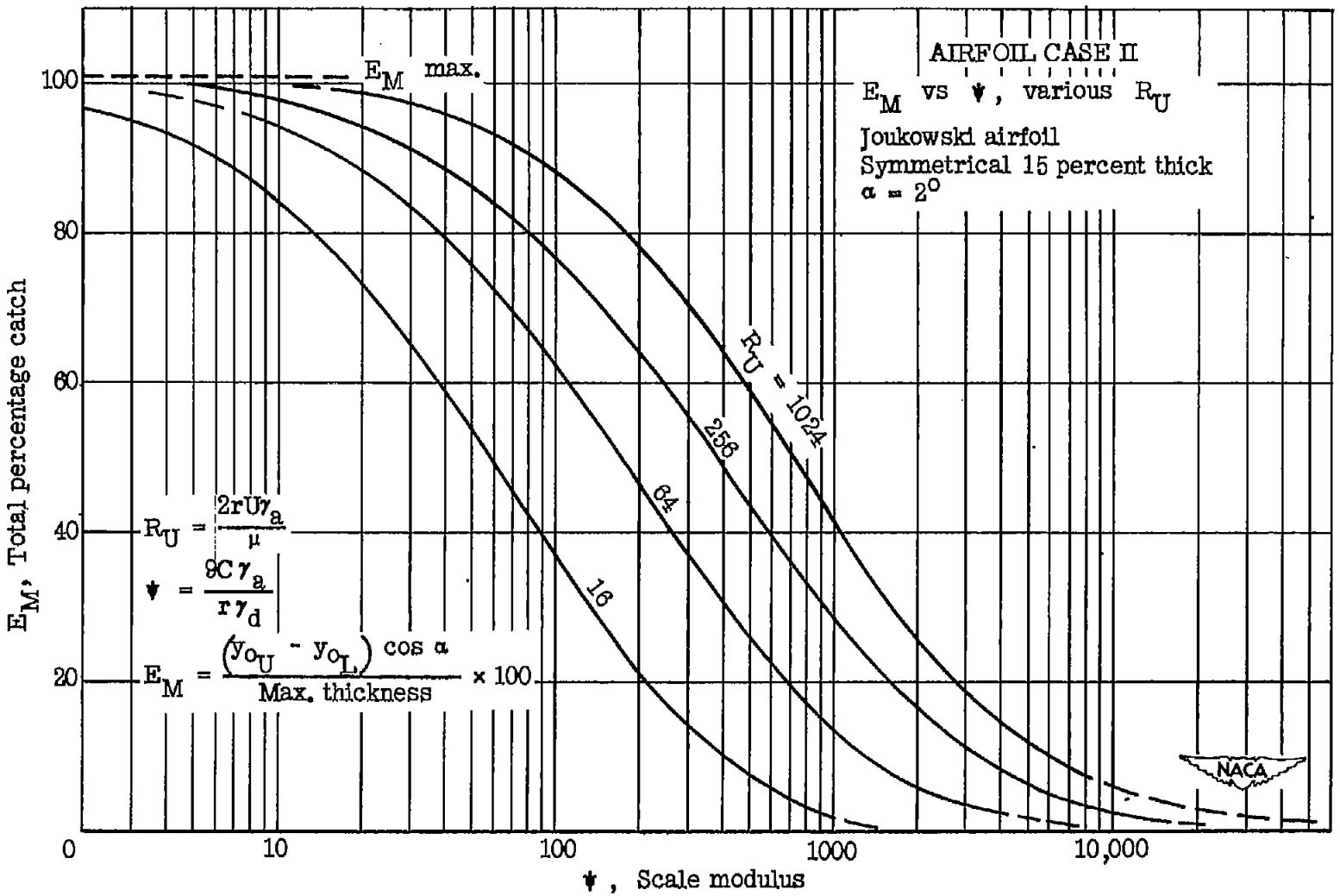
AIRFOIL CASE II
E_M vs Ψ, various R_U
Joukowski airfoil
Symmetrical 15 percent thick
$\alpha = 2^\circ$
E_M max.
$R_U = 1024$
256
64
16
$R_U = \frac{2rU\gamma_a}{\mu}$
$\Psi = \frac{8C\gamma_a}{r\gamma_d}$
$E_M = \frac{(y_{o_U} - y_{o_L}) \cos \alpha}{\text{Max. thickness}} \times 100$
E_M, Total percentage catch
Ψ, Scale modulus
100
80
60
40
20
0
10
100
1000
10,000
NACA

Figure 9.

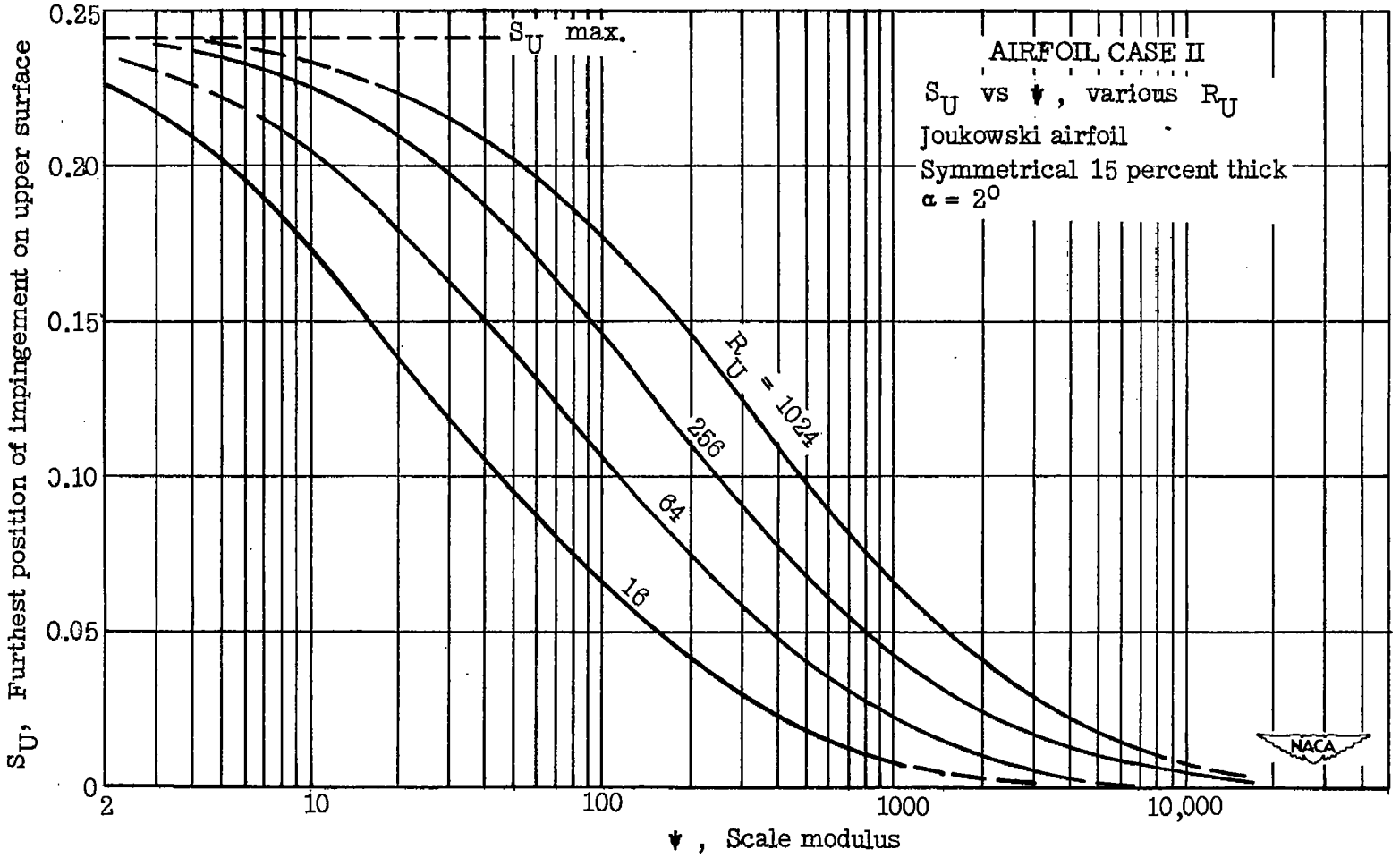
AIRFOIL CASE II
S_U vs Ψ, various R_U
Joukowski airfoil
Symmetrical 15 percent thick
$\alpha = 2^o$
S_U max.
R_U = 1024
256
64
16
S_U, Furthest position of impingement on upper surface
0.25
0.20
0.15
0.10
0.05
0
2
10
100
1000
10,000
Ψ, Scale modulus
NACA

Figure 10.

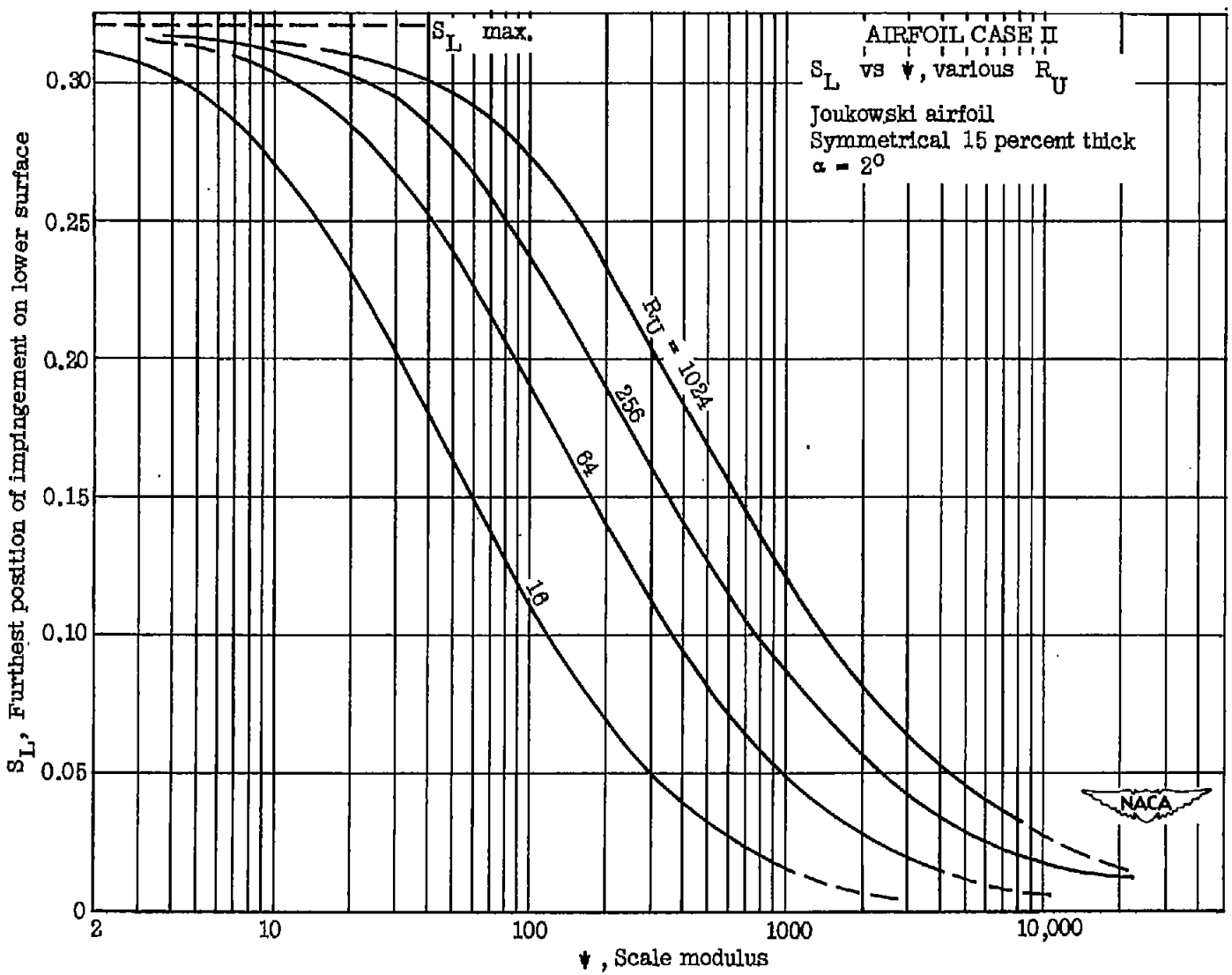
AIRFOIL CASE II
S_L vs ψ, various R_U
Joukowski airfoil
Symmetrical 15 percent thick
$\alpha = 2^0$
S_L max.
R_U = 1024
256
64
16
S_L, Furthest position of impingement on lower surface
0.30
0.25
0.20
0.15
0.10
0.05
0
2
10
100
1000
10,000
ψ, Scale modulus
NACA

Figure 11.

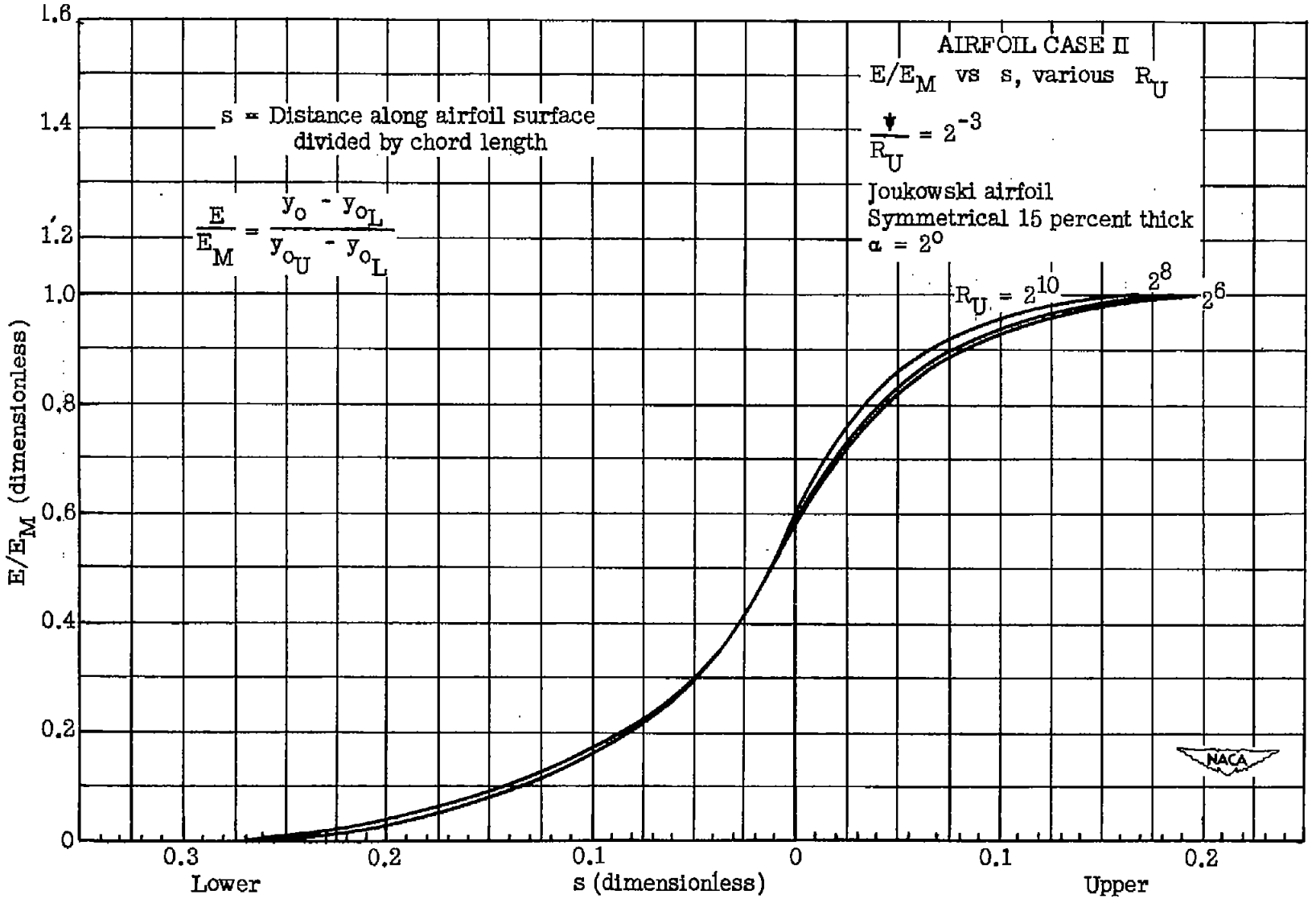
AIRFOIL CASE II
E/E_M vs s, various R_U
t/R_U = 2^-3
Joukowski airfoil
Symmetrical 15 percent thick
α = 2°
s = Distance along airfoil surface divided by chord length
E/E_M = (y_o - y_oL) / (y_oU - y_oL)
R_U = 2^10
2^8
2^6
E/E_M (dimensionless)
1.6
1.4
1.2
1.0
0.8
0.6
0.4
0.2
0
0.3
0.2
0.1
0
0.1
0.2
Lower
s (dimensionless)
Upper
NACA

Figure 12.

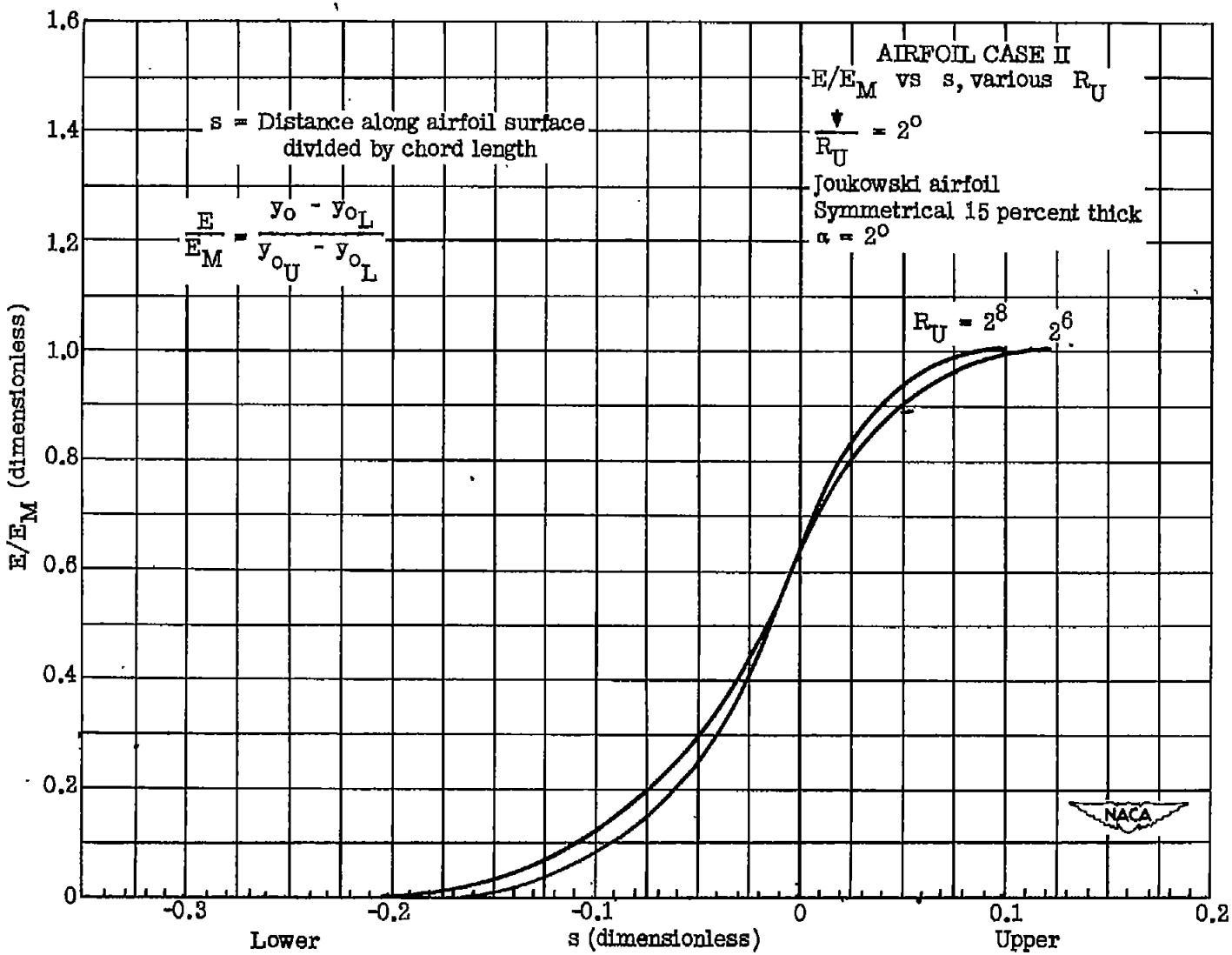
AIRFOIL CASE II
E/E_M vs s, various R_U
↓ / R_U = 2^0
Joukowski airfoil
Symmetrical 15 percent thick
α = 2^0
s = Distance along airfoil surface divided by chord length
E/E_M = (y_o - y_oL) / (y_oU - y_oL)
R_U = 2^8
2^6
E/E_M (dimensionless)
1.6
1.4
1.2
1.0
0.8
0.6
0.4
0.2
0
-0.3
-0.2
-0.1
0
0.1
0.2
Lower
s (dimensionless)
Upper
NACA

Figure 13.

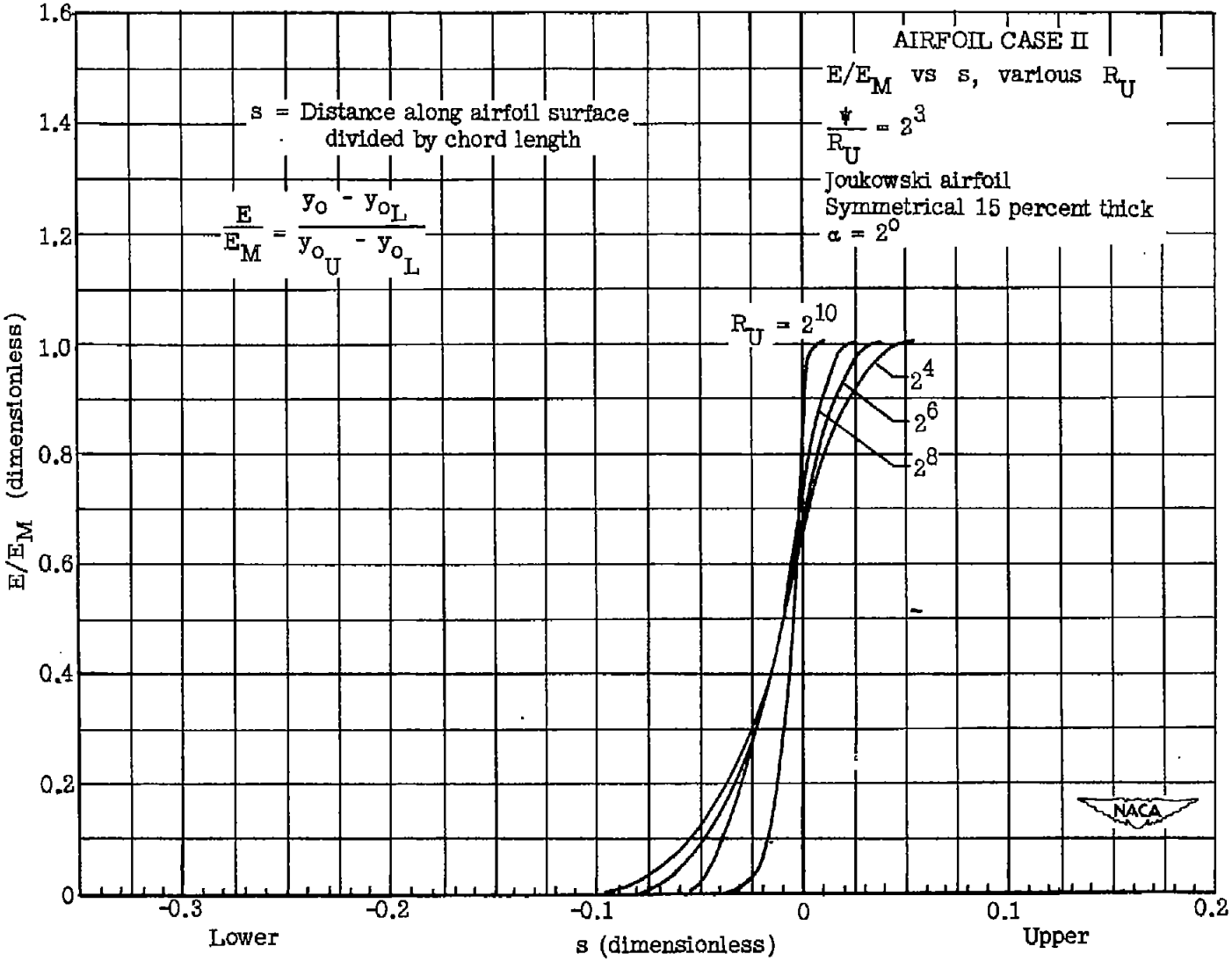
AIRFOIL CASE II
E/E_M vs s, various R_U
t/R_U = 2^3
Joukowski airfoil
Symmetrical 15 percent thick
α = 2°
s = Distance along airfoil surface divided by chord length
E/E_M = (y_o - y_oL) / (y_oU - y_oL)
R_U = 2^10
2^4
2^6
2^8
NACA
E/E_M (dimensionless)
s (dimensionless)
Lower
Upper
1.6
1.4
1.2
1.0
0.8
0.6
0.4
0.2
0
-0.3
-0.2
-0.1
0
0.1
0.2

Figure 14.

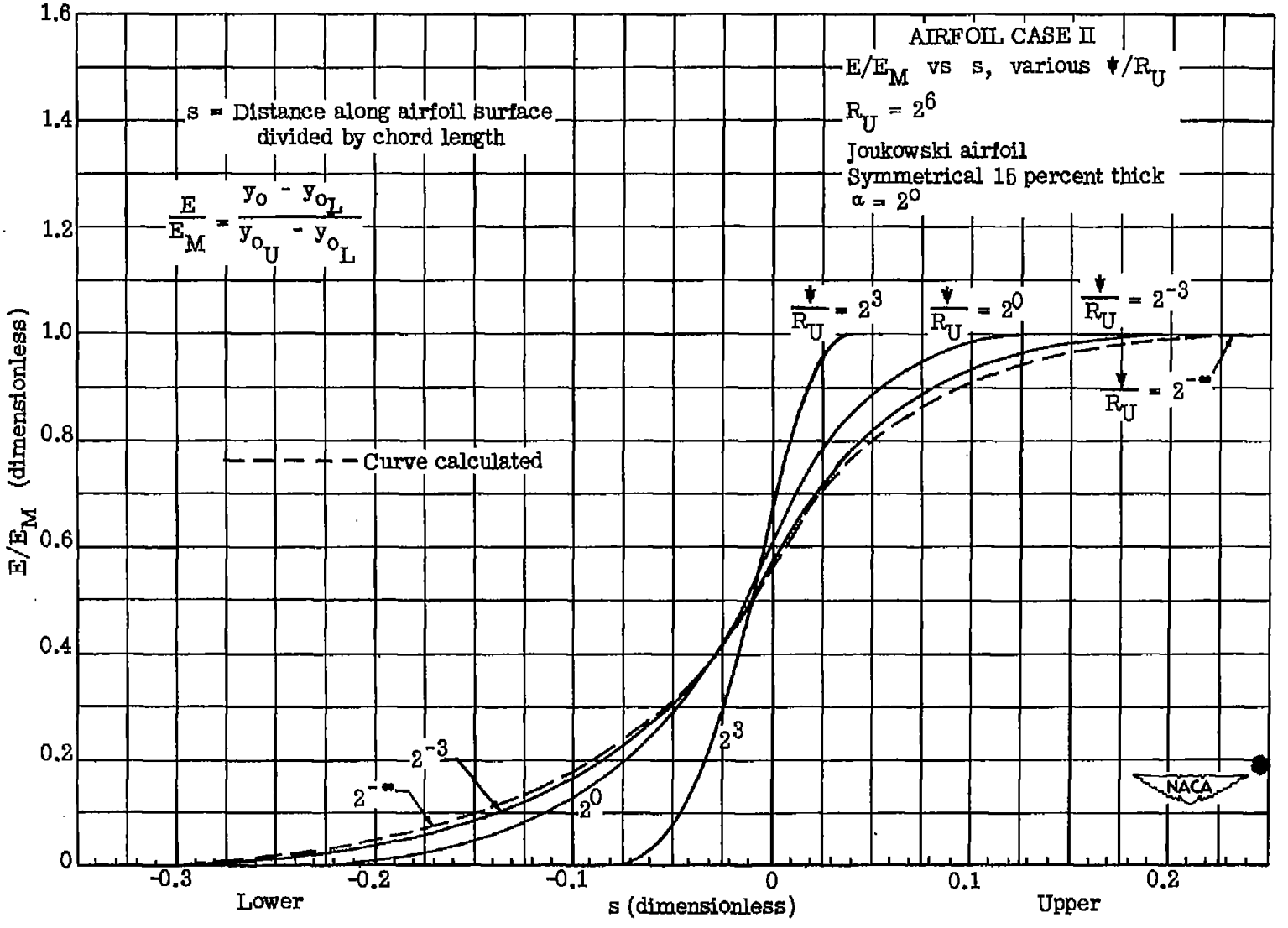
AIRFOIL CASE II
E/E_M vs s, various ↓/R_U
R_U = 2^6
Joukowski airfoil
Symmetrical 15 percent thick
α = 2°
s = Distance along airfoil surface divided by chord length
E/E_M = (y_o - y_oL) / (y_oU - y_oL)
Curve calculated
↓/R_U = 2^3
↓/R_U = 2^0
↓/R_U = 2^-3
↓/R_U = 2^-∞
2^3
2^0
2^-3
2^-∞
NACA
E/E_M (dimensionless)
s (dimensionless)
Lower
Upper
1.6
1.4
1.2
1.0
0.8
0.6
0.4
0.2
0
-0.3
-0.2
-0.1
0
0.1
0.2

Figure 15.

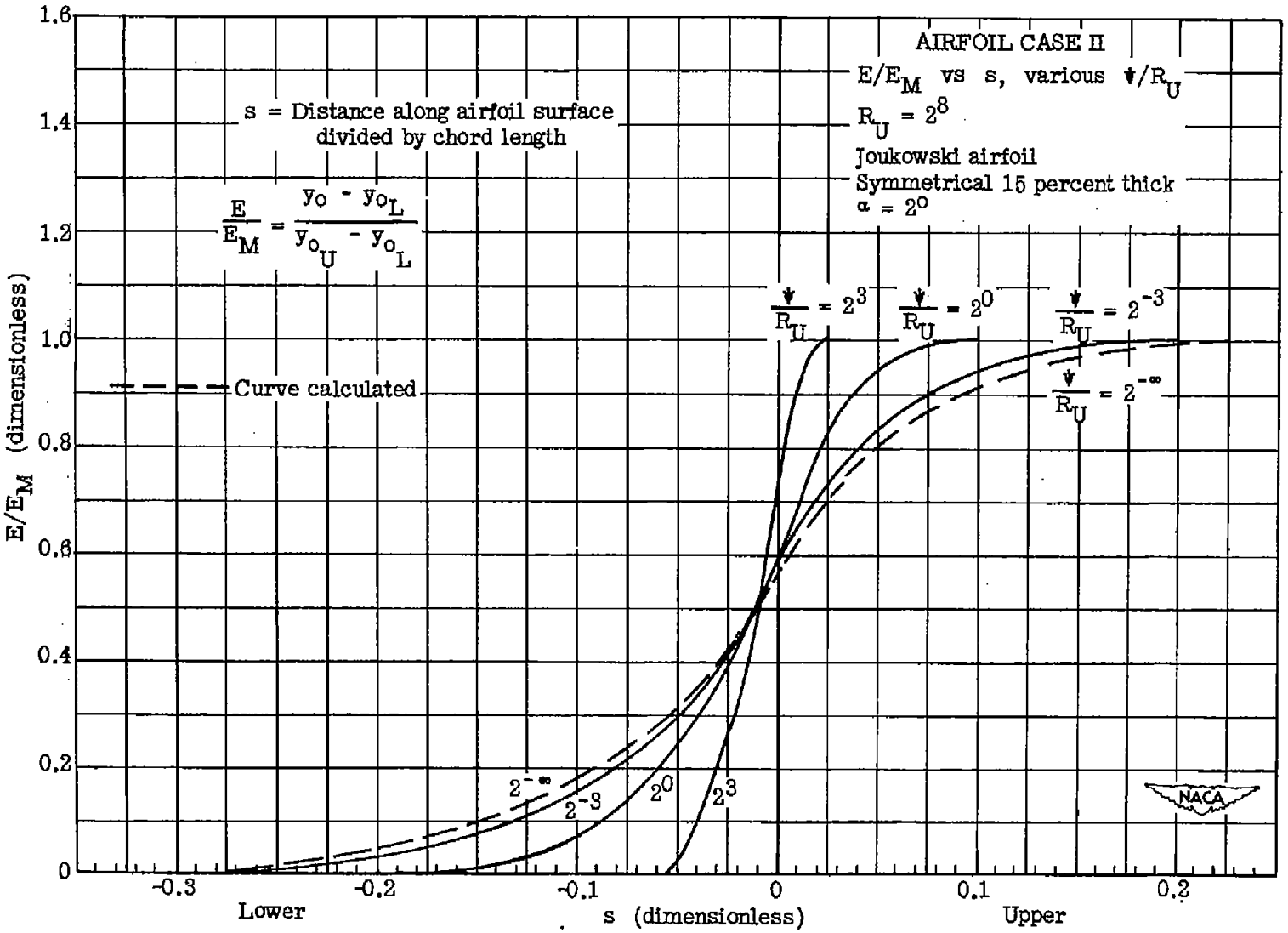
AIRFOIL CASE II
E/E_M vs s, various ψ/R_U
R_U = 2^8
Joukowski airfoil
Symmetrical 15 percent thick
α = 2°
s = Distance along airfoil surface divided by chord length
E/E_M = (y_o - y_oL) / (y_oU - y_oL)
Curve calculated
ψ/R_U = 2^3
ψ/R_U = 2^0
ψ/R_U = 2^-3
ψ/R_U = 2^-∞
2^-∞
2^-3
2^0
2^3
NACA
E/E_M (dimensionless)
s (dimensionless)
Lower
Upper
1.6
1.4
1.2
1.0
0.8
0.6
0.4
0.2
0
-0.3
-0.2
-0.1
0
0.1
0.2

Figure 16.

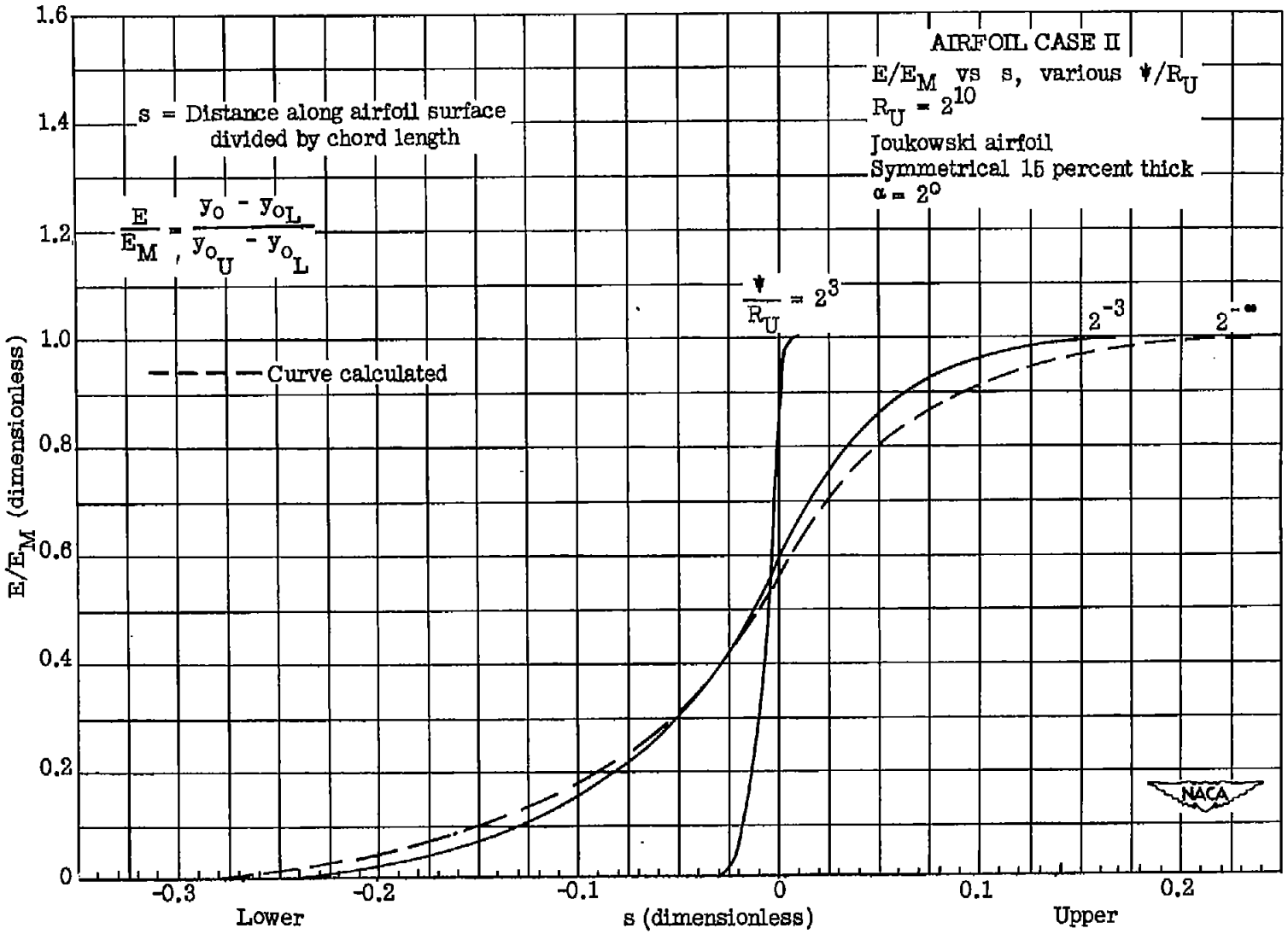
AIRFOIL CASE II
E/E_M vs s, various ψ/R_U
R_U = 2^10
Joukowski airfoil
Symmetrical 15 percent thick
α = 2°
s = Distance along airfoil surface divided by chord length
E/E_M = (y_o - y_oL) / (y_oU - y_oL)
ψ/R_U = 2^3
2^-3
2^-∞
Curve calculated
NACA
E/E_M (dimensionless)
1.6
1.4
1.2
1.0
0.8
0.6
0.4
0.2
0
-0.3
-0.2
-0.1
0
0.1
0.2
Lower
s (dimensionless)
Upper

Figure 17.

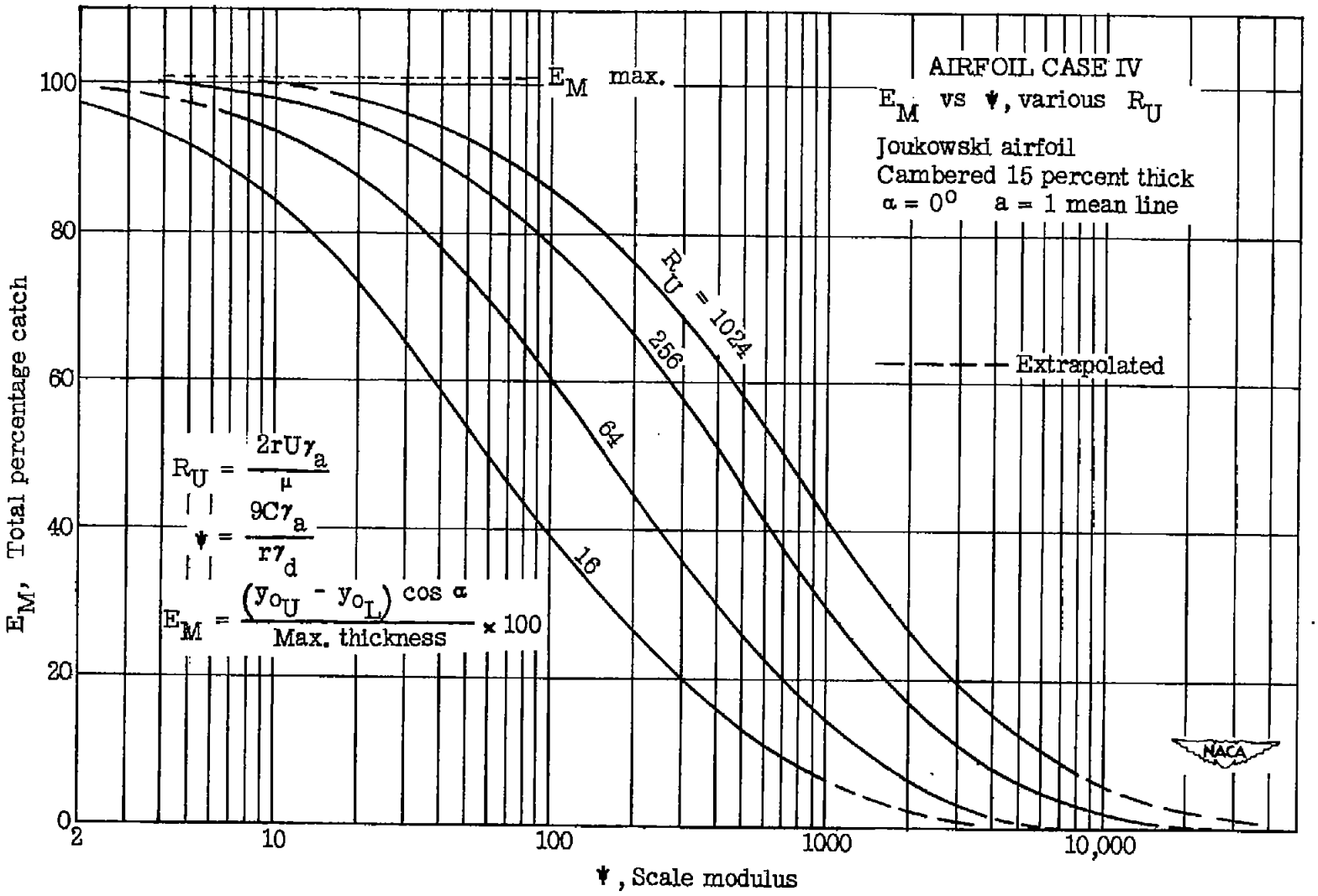
AIRFOIL CASE IV
E_M vs Ψ, various R_U
Joukowski airfoil
Cambered 15 percent thick
$\alpha = 0^\circ$ a = 1 mean line
E_M max.
R_U = 1024
256
64
16
Extrapolated
$R_U = \frac{2rU\gamma_a}{\mu}$
$\Psi = \frac{9C\gamma_a}{r\gamma_d}$
$E_M = \frac{(y_{o_U} - y_{o_L}) \cos \alpha}{\text{Max. thickness}} \times 100$
E_M, Total percentage catch
Ψ, Scale modulus
0
20
40
60
80
100
2
10
100
1000
10,000
NACA

Figure 18.

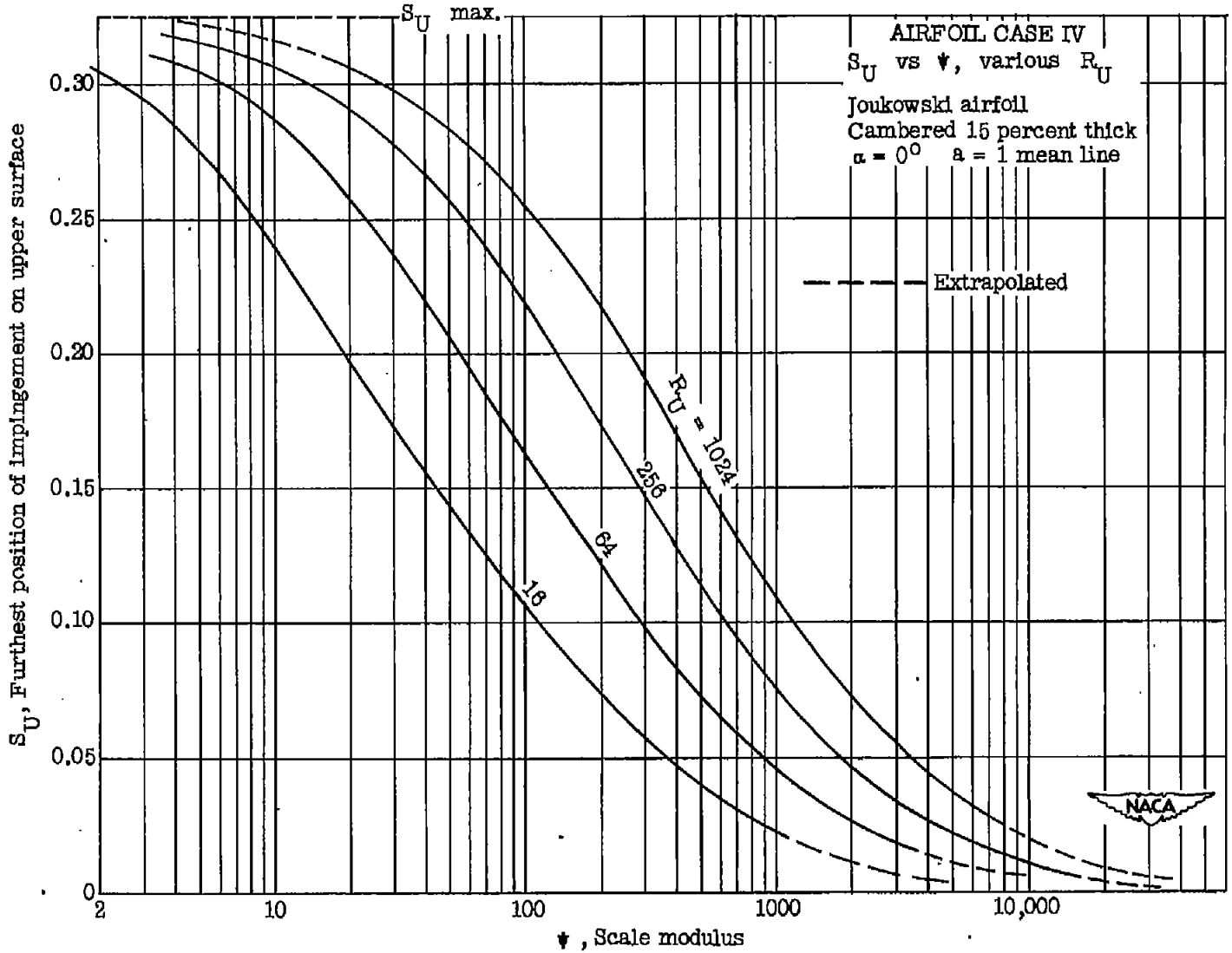
S_U max.
AIRFOIL CASE IV
S_U vs Φ, various R_U
Joukowski airfoil
Cambered 15 percent thick
$\alpha = 0^\circ$ a = 1 mean line
Extrapolated
R_U = 1024
256
64
16
NACA
S_U, Furthest position of impingement on upper surface
0.30
0.25
0.20
0.15
0.10
0.05
0
2
10
100
1000
10,000
Φ, Scale modulus

Figure 19.

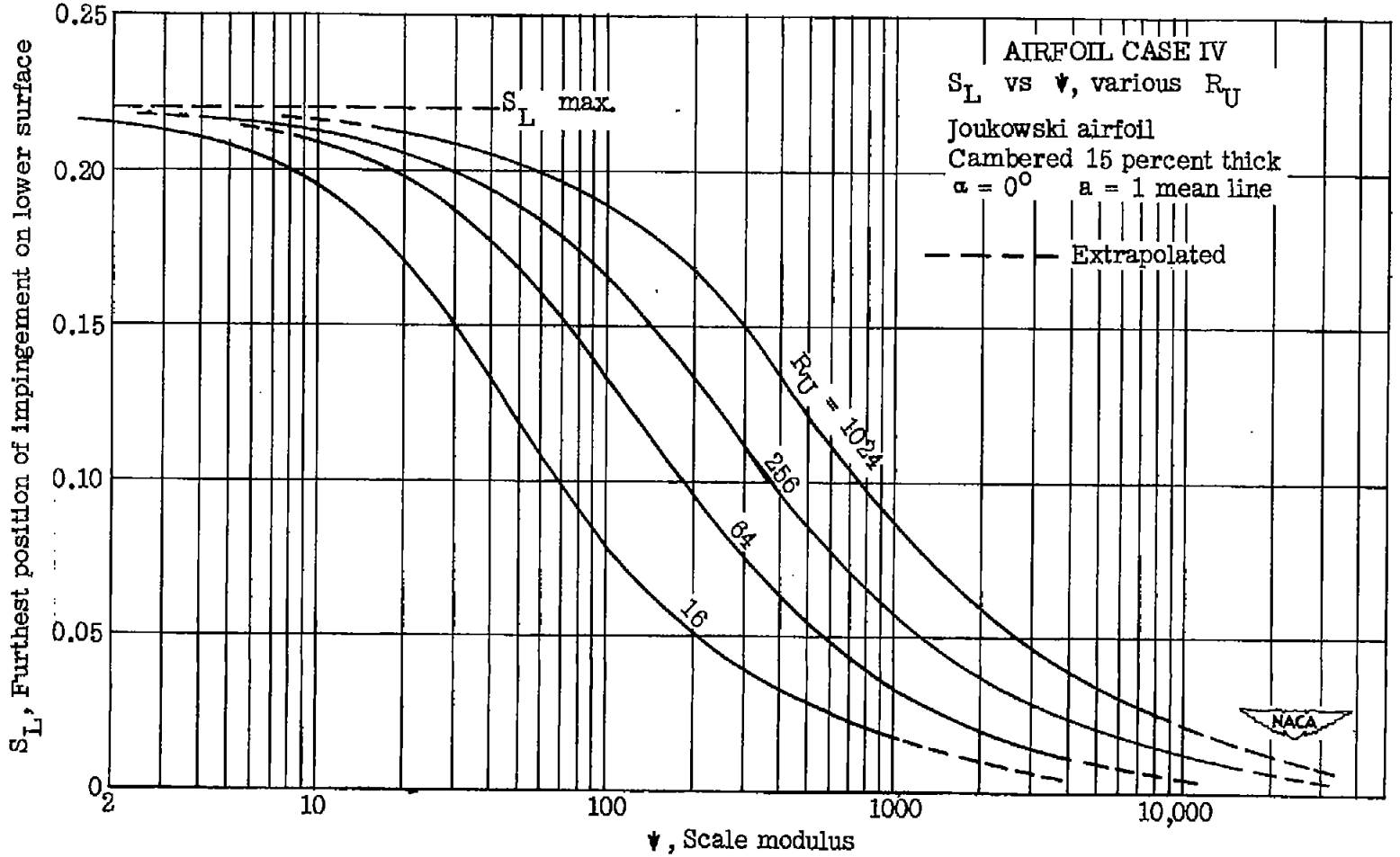
AIRFOIL CASE IV
S_L vs Ψ, various R_U
Joukowski airfoil
Cambered 15 percent thick
$\alpha = 0^\circ$ a = 1 mean line
Extrapolated
S_L max.
R_U = 1024
256
64
16
NACA
S_L, Furthest position of impingement on lower surface
0.25
0.20
0.15
0.10
0.05
0
2
10
100
1000
10,000
Ψ, Scale modulus

Figure 20.

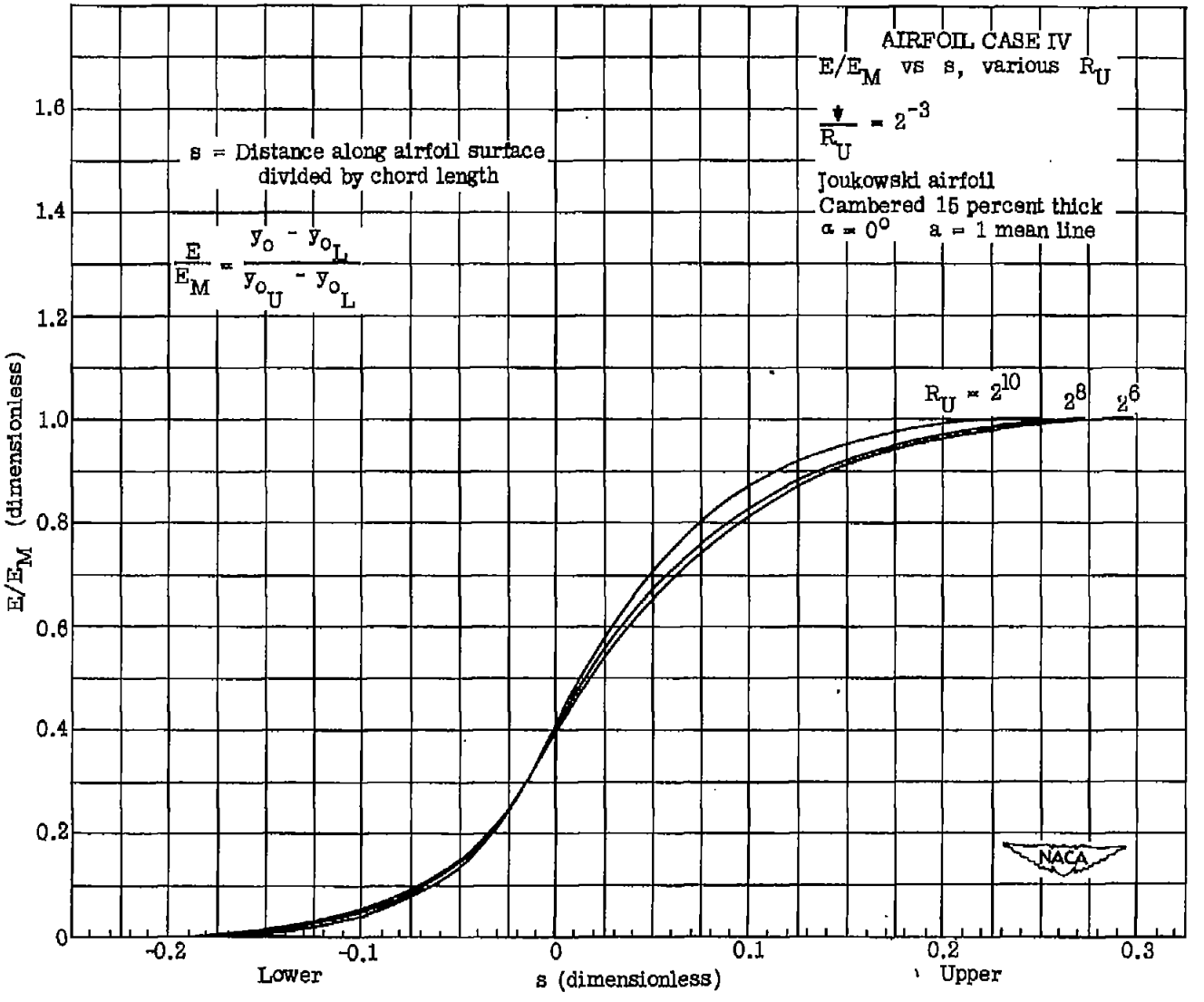
AIRFOIL CASE IV
E/E_M vs s, various R_U
1/R_U = 2^-3
Joukowski airfoil
Cambered 15 percent thick
α = 0° a = 1 mean line
s = Distance along airfoil surface divided by chord length
E/E_M = (y_o - y_oL) / (y_oU - y_oL)
R_U = 2^10
2^8
2^6
NACA
E/E_M (dimensionless)
0
0.2
0.4
0.6
0.8
1.0
1.2
1.4
1.6
-0.2
-0.1
0
0.1
0.2
0.3
Lower
s (dimensionless)
Upper

Figure 21.

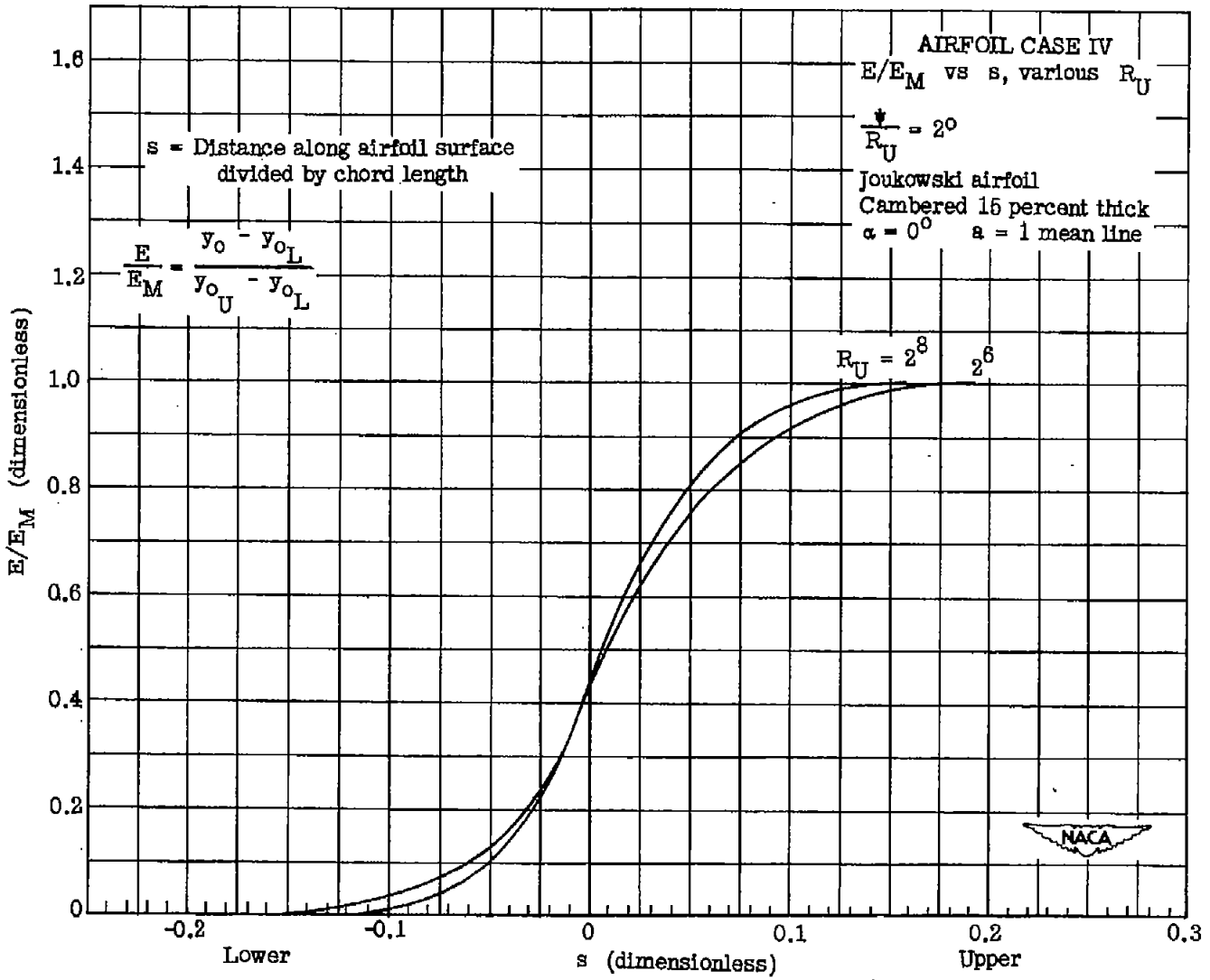
AIRFOIL CASE IV
E/E_M vs s, various R_U
$\frac{\alpha}{R_U} = 2^o$
Joukowski airfoil
Cambered 15 percent thick
$\alpha = 0^o$ a = 1 mean line
s = Distance along airfoil surface divided by chord length
$\frac{E}{E_M} = \frac{y_o - y_{o_L}}{y_{o_U} - y_{o_L}}$
$R_U = 2^8$ 2^6
NACA
E/E_M (dimensionless)
1.6
1.4
1.2
1.0
0.8
0.6
0.4
0.2
0
-0.2
-0.1
0
0.1
0.2
0.3
Lower
s (dimensionless)
Upper

Figure 22.

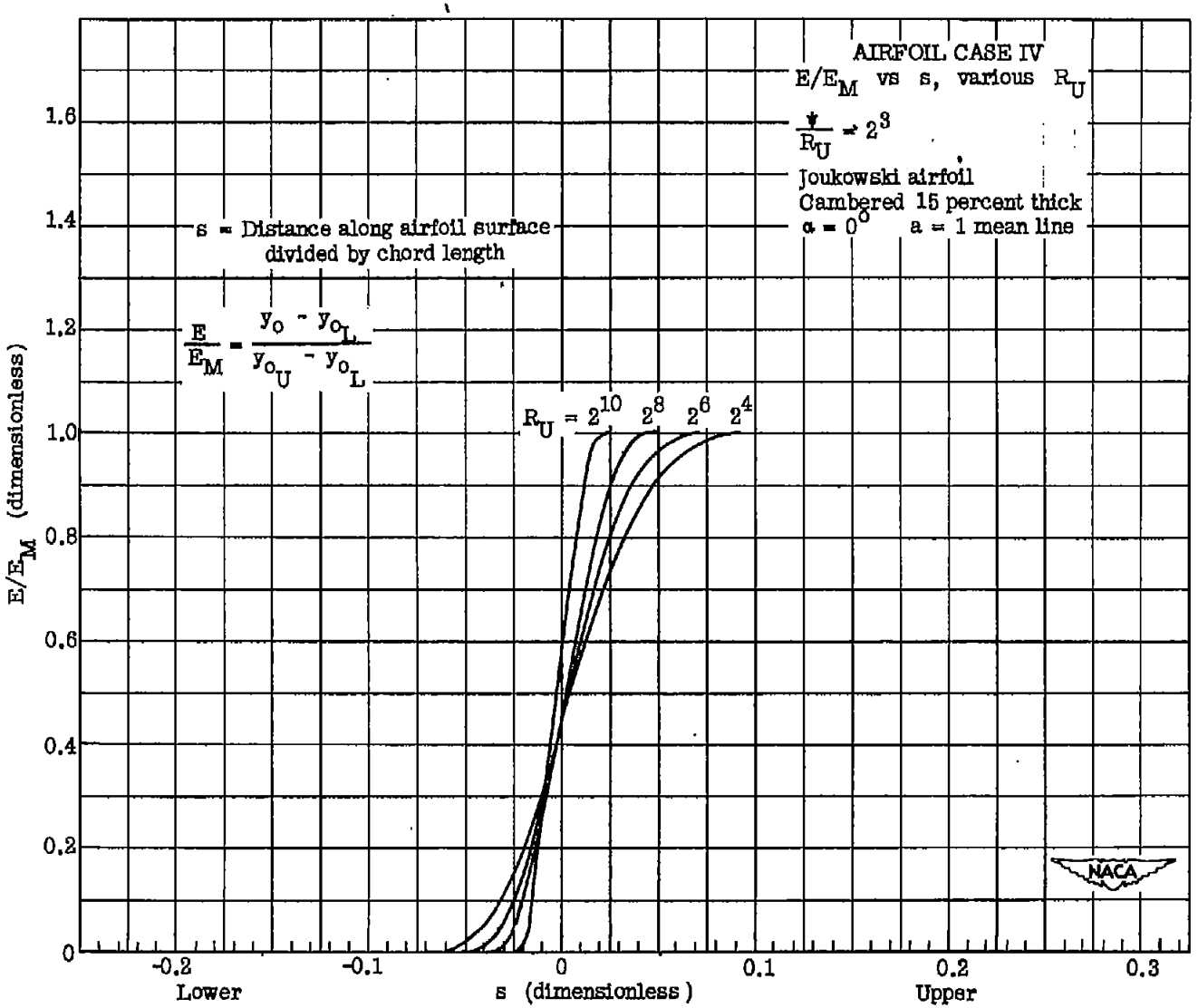
AIRFOIL CASE IV
E/E_M vs s, various R_U
ψ/R_U = 2^3
Joukowski airfoil
Cambered 15 percent thick
α = 0° a = 1 mean line
s = Distance along airfoil surface divided by chord length
E/E_M = (y_o - y_oL) / (y_oU - y_oL)
R_U = 2^10 2^8 2^6 2^4
E/E_M (dimensionless)
1.6
1.4
1.2
1.0
0.8
0.6
0.4
0.2
0
-0.2
-0.1
0
0.1
0.2
0.3
Lower
s (dimensionless)
Upper
NACA

Figure 23.

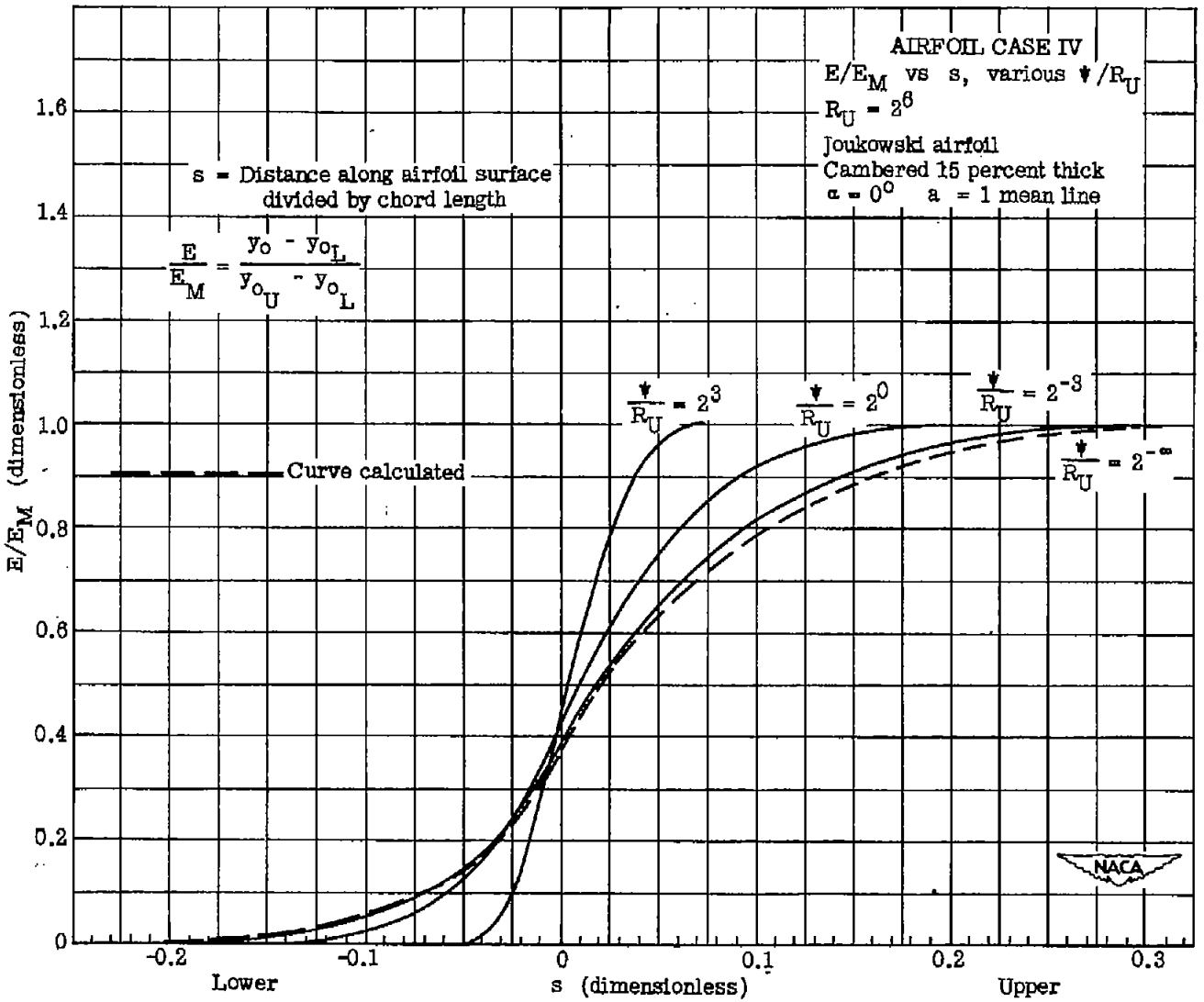
AIRFOIL CASE IV
E/E_M vs s, various ψ/R_U
R_U = 2^6
Joukowski airfoil
Cambered 15 percent thick
α = 0° a = 1 mean line
s = Distance along airfoil surface divided by chord length
E/E_M = (y_o - y_oL) / (y_oU - y_oL)
Curve calculated
ψ/R_U = 2^3
ψ/R_U = 2^0
ψ/R_U = 2^-3
ψ/R_U = 2^-∞
NACA
E/E_M (dimensionless)
1.6
1.4
1.2
1.0
0.8
0.6
0.4
0.2
0
-0.2
-0.1
0
0.1
0.2
0.3
Lower
s (dimensionless)
Upper

Figure 24.

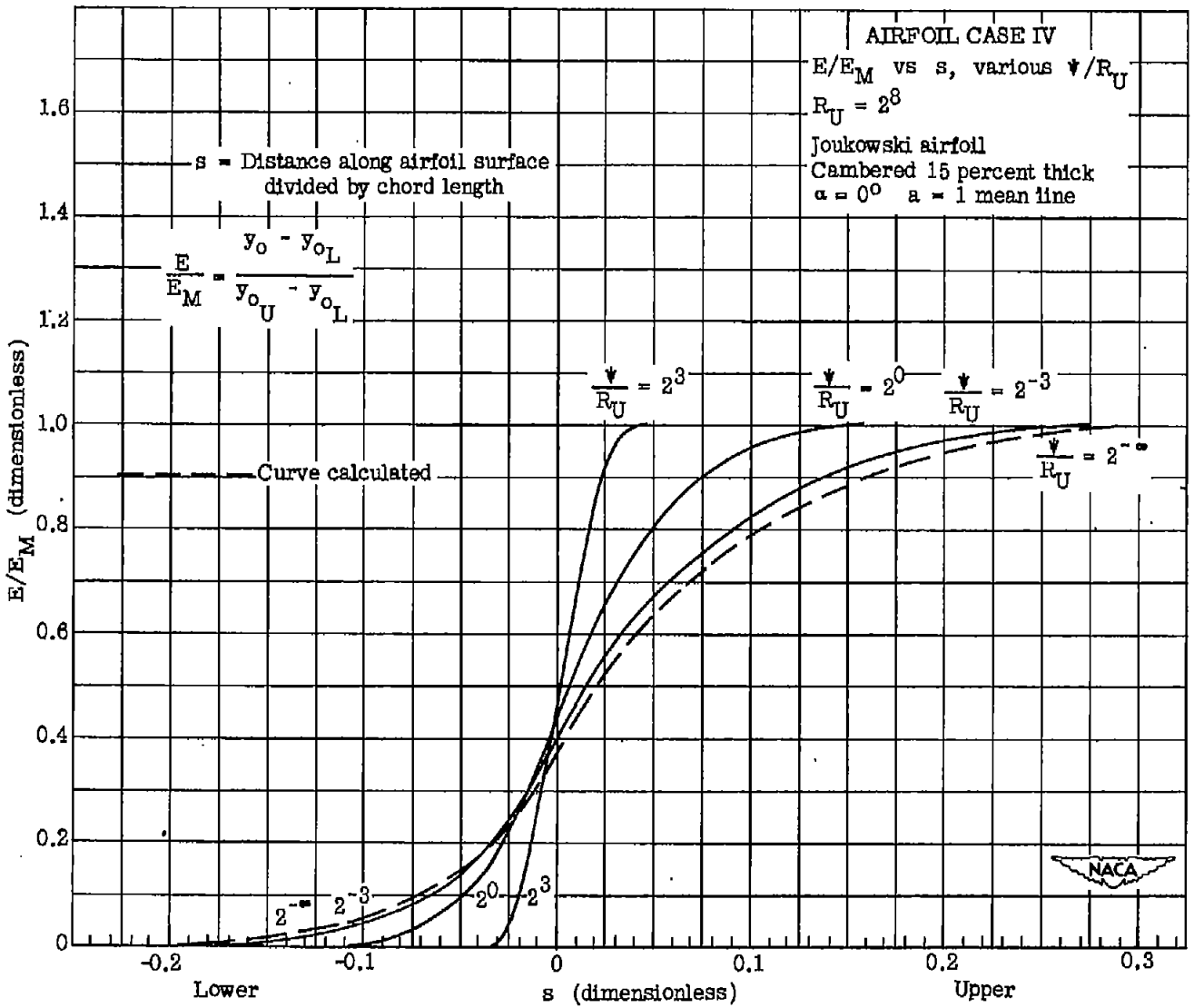
AIRFOIL CASE IV
E/E_M vs s, various ψ/R_U
R_U = 2^8
Joukowski airfoil
Cambered 15 percent thick
α = 0° a = 1 mean line
s = Distance along airfoil surface divided by chord length
E/E_M = (y_o - y_oL) / (y_oU - y_oL)
Curve calculated
ψ/R_U = 2^3
ψ/R_U = 2^0
ψ/R_U = 2^-3
ψ/R_U = 2^-∞
2^-∞
2^-3
2^0
2^3
NACA
E/E_M (dimensionless)
1.6
1.4
1.2
1.0
0.8
0.6
0.4
0.2
0
-0.2
-0.1
0
0.1
0.2
0.3
Lower
s (dimensionless)
Upper

Figure 25.

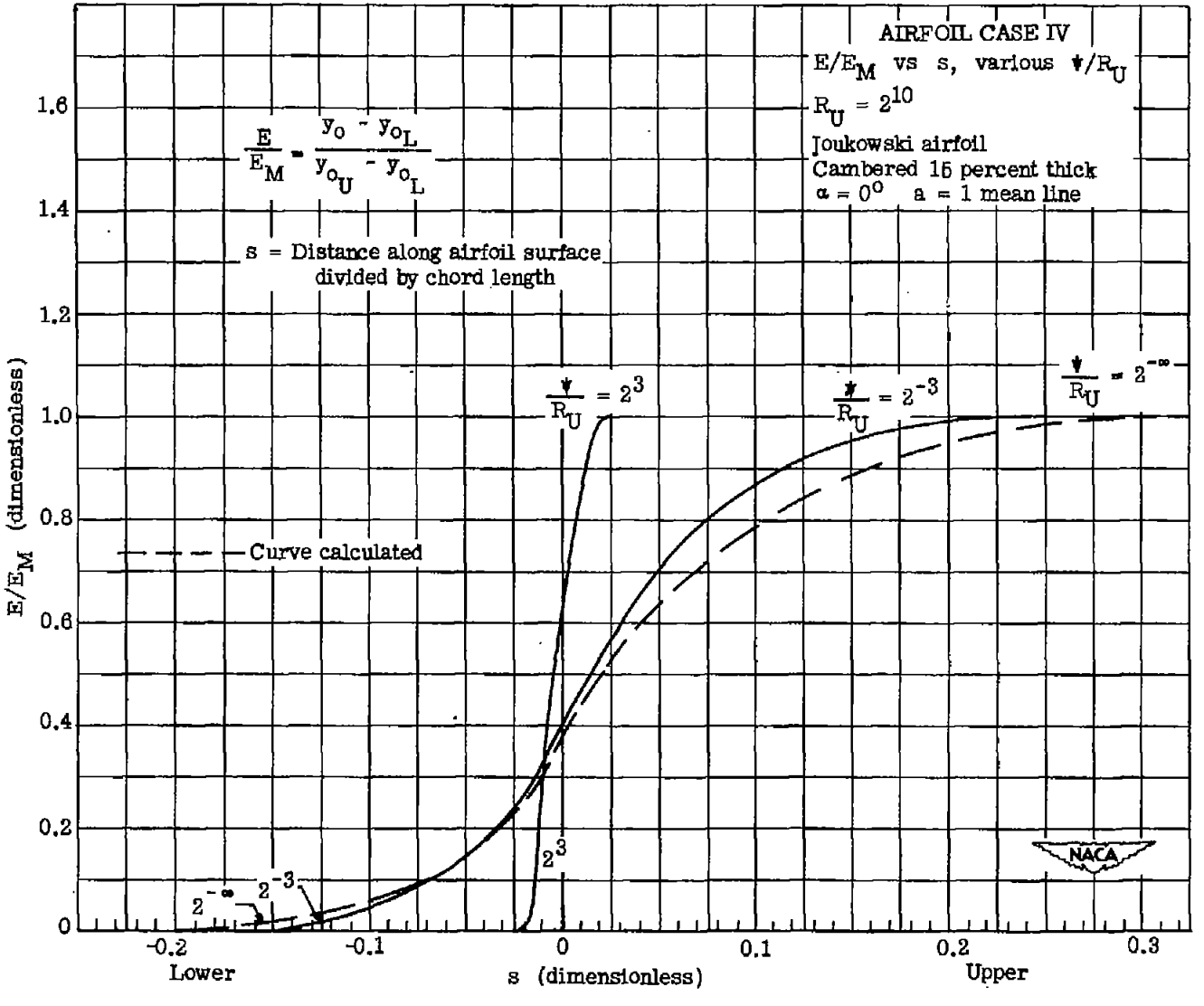
AIRFOIL CASE IV
E/E_M vs s, various ψ/R_U
R_U = 2^10
Joukowski airfoil
Cambered 15 percent thick
α = 0° a = 1 mean line
E/E_M = (y_o - y_oL) / (y_oU - y_oL)
s = Distance along airfoil surface divided by chord length
ψ/R_U = 2^3
ψ/R_U = 2^-3
ψ/R_U = 2^-∞
Curve calculated
2^3
2^-3
2^-∞
NACA
E/E_M (dimensionless)
s (dimensionless)
Lower
Upper
0
0.2
0.4
0.6
0.8
1.0
1.2
1.4
1.6
-0.2
-0.1
0
0.1
0.2
0.3

Figure 28.

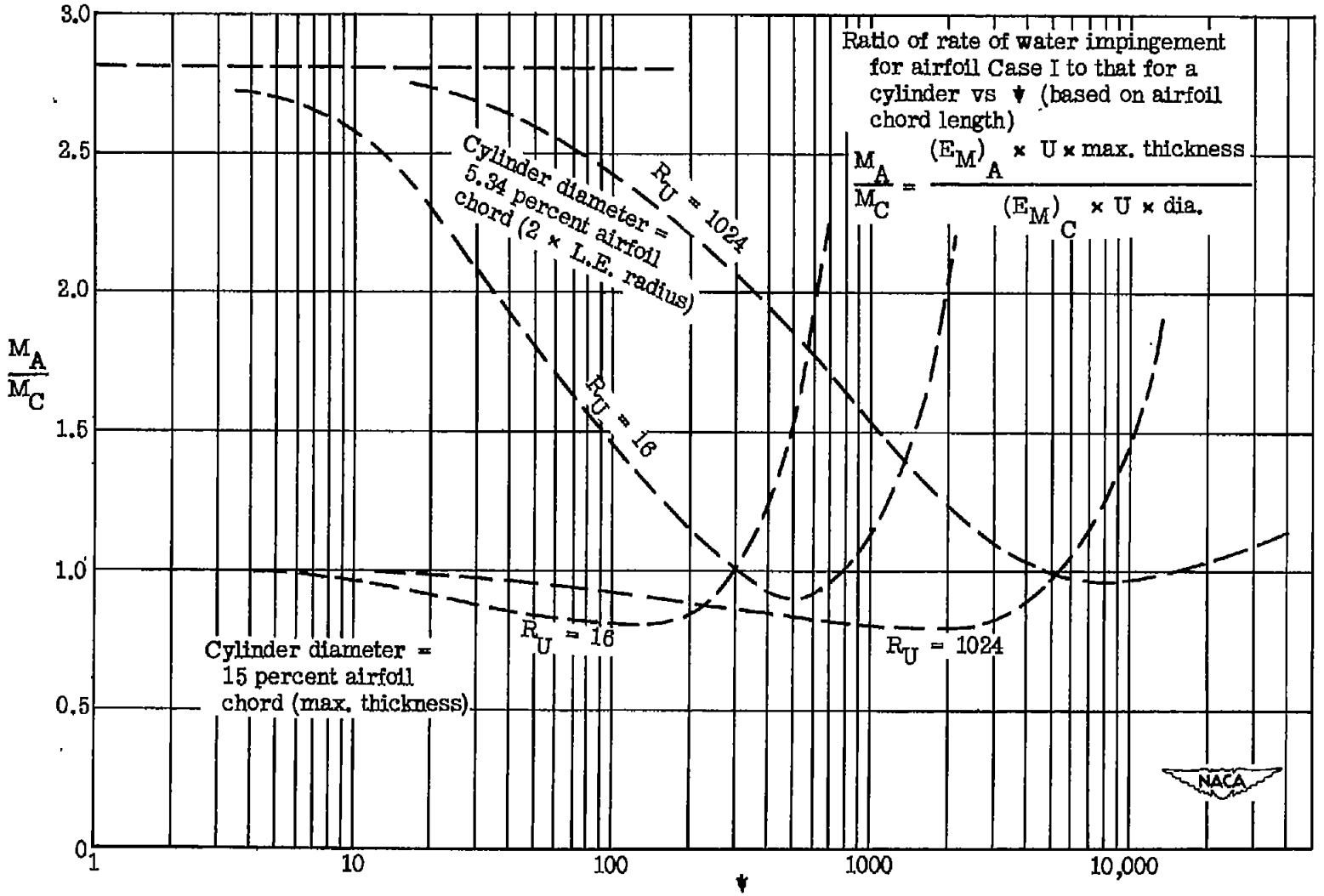
Ratio of rate of water impingement for airfoil Case I to that for a cylinder vs ϕ (based on airfoil chord length)
$\frac{M_A}{M_C} = \frac{(E_M)_A \times U \times \text{max. thickness}}{(E_M)_C \times U \times \text{dia.}}$
$\frac{M_A}{M_C}$
3.0
2.5
2.0
1.5
1.0
0.5
0
1
10
100
1000
10,000
ϕ
Cylinder diameter = 5.34 percent airfoil chord (2 × L.E. radius)
R_U = 1024
R_U = 16
Cylinder diameter = 15 percent airfoil chord (max. thickness)
R_U = 16
R_U = 1024
NACA

Figure 27.

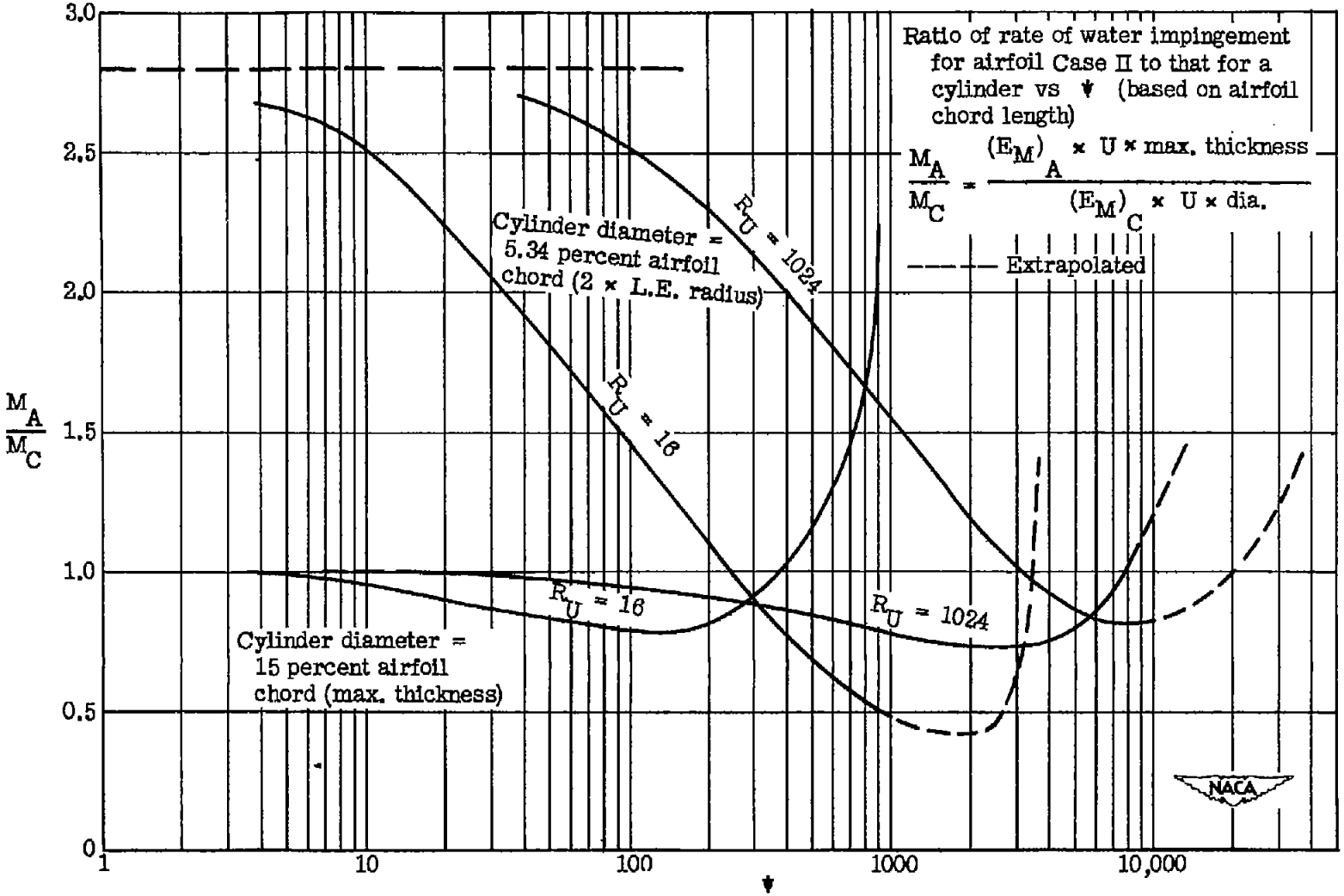
Ratio of rate of water impingement for airfoil Case II to that for a cylinder vs ϕ (based on airfoil chord length)
$\frac{M_A}{M_C} = \frac{(E_M)_A \times U \times \text{max. thickness}}{(E_M)_C \times U \times \text{dia.}}$
Extrapolated
Cylinder diameter = 5.34 percent airfoil chord (2 × L.E. radius)
Cylinder diameter = 15 percent airfoil chord (max. thickness)
R_U = 1024
R_U = 16
R_U = 16
R_U = 1024
$\frac{M_A}{M_C}$
ϕ
3.0
2.5
2.0
1.5
1.0
0.5
0
1
10
100
1000
10,000
NACA

Figure 28.

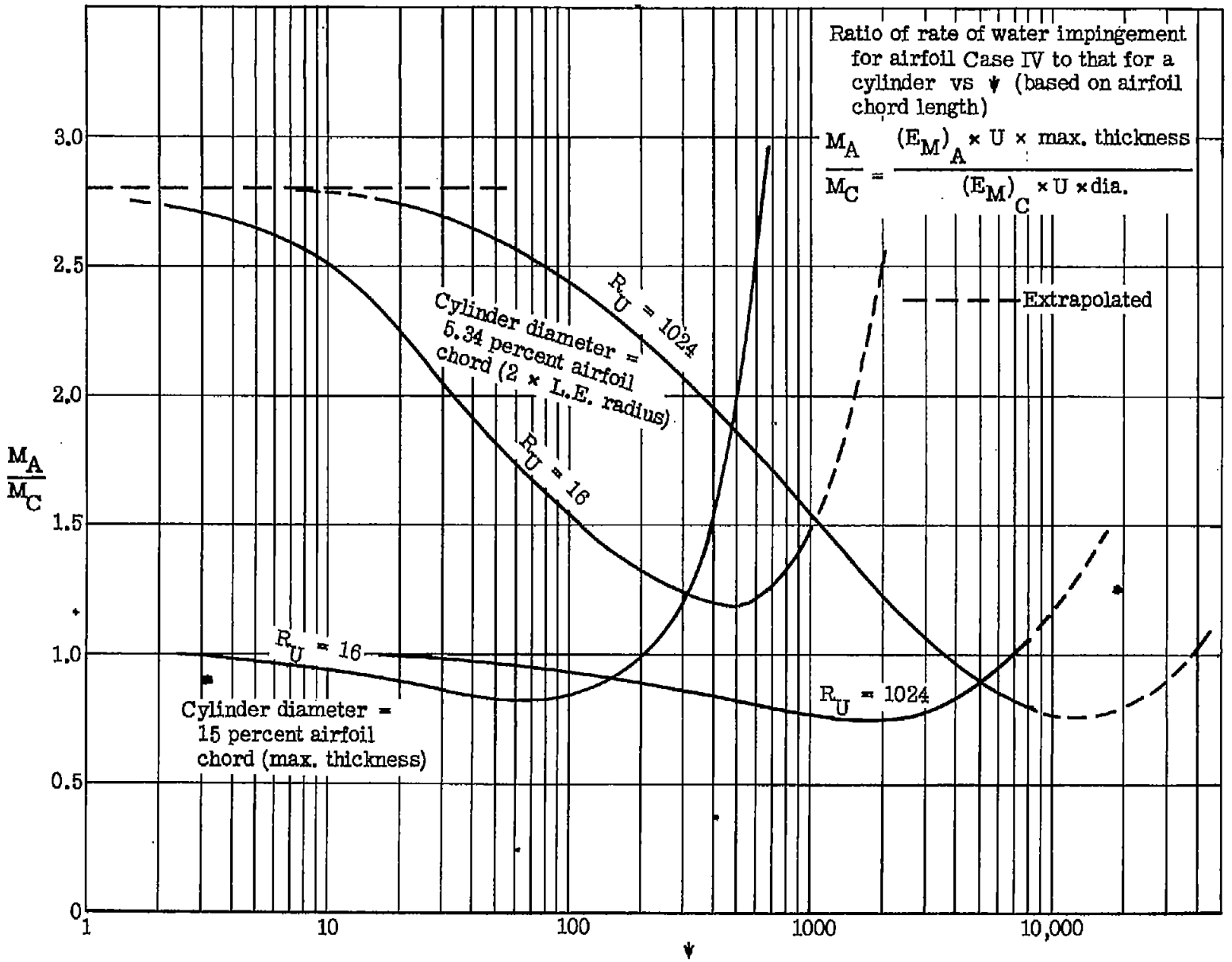
Ratio of rate of water impingement for airfoil Case IV to that for a cylinder vs ψ (based on airfoil chord length)
$\frac{M_A}{M_C} = \frac{(E_M)_A \times U \times \text{max. thickness}}{(E_M)_C \times U \times \text{dia.}}$
Extrapolated
R_U = 1024
Cylinder diameter = 5.34 percent airfoil chord (2 × L.E. radius)
R_U = 16
R_U = 16
Cylinder diameter = 15 percent airfoil chord (max. thickness)
R_U = 1024
$\frac{M_A}{M_C}$
3.0
2.5
2.0
1.5
1.0
0.5
0
1
10
100
1000
10,000
ψ

Figure 29.